

RADIO LOUD AND RADIO QUIET ACTIVE GALACTIC NUCLEI

Chun Xu¹, Mario Livio and Stefi Baum

Space Telescope Science Institute

3700 San Martin Drive

Baltimore, MD 21218

chunxu@stsci.edu, mlivio@stsci.edu, sbaum@stsci.edu

Received _____; accepted _____

arXiv:astro-ph/9905322v1 25 May 1999

¹Also at: Department of Astronomy, University of Maryland, College Park, MD 20742

ABSTRACT

We generated a sample of 409 AGNs for which both the radio luminosity at 5 GHz and the line luminosity in [OIII] 5007 have been measured. The radio luminosity spans a range of ten orders of magnitude, and the [OIII] line luminosity spans a range of eight orders of magnitude — both considerably larger than the ranges in previous studies. We show that these two quantities are correlated in a similar way for both radio-loud and radio-quiet AGNs. We demonstrate that the observed correlation can be explained in terms of a model in which jets are accelerated and collimated by a vertical magnetic field.

Subject headings: galaxies: active — galaxies: nuclei — galaxies: spiral — galaxies: elliptical — quasars: general — radio continuum: galaxies

1. INTRODUCTION

The “unified” scheme of active galactic nuclei (AGNs) has been very successful in explaining a variety of AGN properties on the basis of the viewing angle θ (see *e.g.*, review by Urry & Padovani 1995). It is very clear, however, that more physical parameters are required to construct a truly “unified” model of all AGNs (*e.g.*, Blandford 1990). In particular, it is by now well established that AGNs fall into two families in terms of their radio power (as measured for example by their 5 GHz luminosities), the “radio-loud” and “radio-quiet” AGNs (*e.g.*, Baum & Heckman 1989; Miller, Rawlings & Saunders 1993). Phenomenologically, radio-louds are always associated with large scale radio jets and lobes while the radio-quiet ones have very little or weak radio emitting ejecta. Radio-loud AGNs are almost always associated with early type galaxies, while the radio-quiet ones are mostly found in spirals and S0s.

One of the ways to tackle observationally the question of the additional fundamental parameters (other than the viewing angle θ), is to examine the AGN luminosities in a variety of wavebands. In particular, it has been shown that a correlation exists between the radio luminosity ($L_{5\text{ GHz}}$) and the [OIII] 5007 narrow line luminosity ($L_{[\text{OIII}]}$) (*e.g.*, Rawlings & Saunders 1991; Baum & Heckman 1989).

In the present work, we study the $L_{5\text{ GHz}}-L_{[\text{OIII}]}$ and related correlations for a much larger data set, covering a very wide range of luminosities. We then use the obtained results in combination with recent theoretical developments in an attempt to place constraints on possible scenarios for the nature of radio-loud and radio-quiet AGNs.

In Section 2 we describe the samples used and the data. The results are presented in Section 3, and discussed in Section 4. A summary and conclusions follow.

2. SAMPLES AND DATA HANDLING

All the data were compiled from the literature and through the NASA Extragalactic Database (NED). Our original sample included four categories of AGNs: (1) Radio sources (Bennett 1962; Smith & Spinrad 1980; Zirbel & Baum 1995; Condon, Frayer & Broderick 1991), (2) Seyfert galaxies (Lipovetsky, Neizvestung & Neizvestnara 1988; Dahari & Robertis 1988; Whittle 1992), (3) BL Lac objects (Veron-Cetty & Veron 1996; Padovani & Giommi 1995), and (4) Quasars (Schmidt & Green 1983; Brotherton 1996; Boroson & Green 1992). To these we added many sources found individually in the literature, thus generating a sample of about 2,000 AGNs. From this sample we selected all the objects for which measurements of both the radio luminosity at 5 GHz and the luminosity in the [OIII] 5007 forbidden line existed. We have thus generated a sample of 409 sources, including: 162 Seyfert galaxies, 136 quasars, 107 radio galaxies and 4 BL Lac objects.

Table 1 gives a list of all the sources used, with the relevant information for each object. Specifically, we list in columns 1–6 respectively the object’s IAU name, its catalogue name, its identification (a galaxy (G) or a quasar (Q)), the nature of its activity: Seyfert or Radio Galaxy, its morphology type and its redshift. In columns 7–10 we list respectively: its luminosity in the [OIII] 5007 line, the total radio power at 5 GHz, the core radio power at 5 GHz, the x-ray luminosity in the 2–10 keV band and the corresponding references. In the last column (column 15) we remark if the object is regarded as radio-loud (L) or radio-quiet (Q) in our study. A more detailed notation is attached at the end of Table 1. Almost all the data presented on the luminosities represent actual measurements, with very few (*e.g.*, core radio powers from Zirbel & Baum 1995) upper and lower limits. As a rule, if a certain quantity was found to have several different quoted values, the one closest to the mean was taken.

The radio powers at 5 GHz given in Table 1 were either taken directly from the

literature, or calculated from the given fluxes. A value of the Hubble constant of $H_0 = 50 \text{ km s}^{-1} \text{ Mpc}^{-1}$ has been assumed throughout. In calculating the radio power of sources for which the spectral index was not available (assuming a power law $S_\nu \propto \nu^{-\alpha}$), a mean index of 0.75 was adopted.

The luminosities in the [OIII] 5007 line were mostly calculated from the fluxes found in the literature (without reddening corrections, since very few of the latter are available, *e.g.*, Koski 1978). In a case in which only the combined fluxes of [OIII] 5007 and 4959 were given (Steiner 1981), the flux in the 5007 line was taken to be 3/4 of the combined flux. In two cases in which only equivalent widths of [OIII] 5007 were given (Brotherton 1996; Boroson & Green 1992), the continua were determined from the corresponding spectra.

The x-ray luminosities in the 2–10 keV band were calculated from the integrated fluxes. In a case in which only the HEAO/A-2 count rates was given (Ceca *et. al.* 1990), the fluxes were calculated assuming a mean energy index of 0.65.

The redshifts were obtained from the literature and cross checked through the NED.

While clearly the use of many sources for the data makes our sample inhomogeneous in terms of the errors involved, this has a very little effect on our conclusions, since the data now span 8 orders of magnitudes in the [OIII] luminosity and 10 orders of magnitude in the radio luminosity.

3. ANALYSIS AND RESULTS

In Fig. 1, we present the radio luminosity at 5 GHz, $L_{5 \text{ GHz}}$, as a function of the [OIII] 5007 line luminosity, $L_{[\text{OIII}]}$, for all the sources in our sample. The separation into the two families of radio-loud and radio-quiet AGNs with a significant gap between them is immediately apparent. The radio luminosities are different by a factor 10^3 – 10^4 between the

two groups (at a given [OIII] luminosity). We do find a small group ($\sim 3\%$ of the sample) of objects which appear to occupy the region between the two main families. These tentative “intermediate” objects have been represented by filled circles in Fig. 1.

Linear fits to the radio-loud and radio-quiet AGNs (excluding the intermediate objects) give:

$$\begin{aligned} \log(L_{5\text{ GHz}}) &= (0.61 \pm 0.07) \log(L_{[\text{OIII}]}) + (3.7 \pm 0.6) \text{ radio loud} \\ \log(L_{5\text{ GHz}}) &= (0.45 \pm 0.07) \log(L_{[\text{OIII}]}) + (5.6 \pm 0.6) \text{ radio quiet} \end{aligned} \quad (1)$$

Here, $L_{5\text{ GHz}}$ is the radio luminosity in Watts $\text{Hz}^{-1} \text{Sr}^{-1}$, and $L_{[\text{OIII}]}$ is the [OIII] line luminosity in Watts. In determining whether an object belongs to the radio-loud, radio-quiet or intermediate group, we first selected out two distinct groups of objects (namely radio-louds and radio-quiet) based on the distribution in the $L_{5\text{GHz}}-L_{[\text{OIII}]}$ diagram (Fig. 1). We then found linear fits to the two groups respectively. We considered the objects whose radio luminosities (at 5 GHz) are higher than the “radio-loud” fitting minus 2.75σ as radio-loud, those whose radio luminosities are less than the “radio-quiet” fitting plus 2.5σ as radio-quiet, and those which lie between the two groups as intermediate. This way of defining radio-loud and radio-quiet is to some extent semi-empirical. The reason we chose slightly different criteria in determining the radio-loud and radio-quiet membership was to achieve the best visual representation of the two groups in Fig. 1.

We note that the samples used by previous authors (*e.g.*, radio quiet quasars by Miller *et. al.* 1993, radio-loud objects by Rawlings 1994) represent sub-groups of our sample. These authors found a relation with a somewhat steeper slope ($\sim 0.85-1.0$) for the subgroups.

In Fig. 2a, we present the same data, now indicating the different classes of AGNs (note that a few of the objects might have been misclassified in the literature). What becomes immediately clear from this figure is that by plotting $L_{5\text{ GHz}}$ vs. $L_{[\text{OIII}]}$ only for some *individual classes* of AGNs (*e.g.*, quasars), one could obtain a distribution of

points that would have looked like a relation with a rather different slope (see Fig. 2b). In such a case it would have been difficult to determine whether this indeed represents a different functional dependence of $L_{5\text{ GHz}}$ or $L_{[\text{OIII}]}$, or whether this is merely an artifact of examining, for example, only the rightmost edges of two separate linear relations (as in the case of quasars, Figs. 2a, 2b). For the moment we will assume that the latter interpretation is correct, since our basic assumption is one of an underlying “unified” scheme. We do note however that extreme caution should be exercised in attempts to determine the properties of subclasses of AGNs, and that in principle, the former interpretation may be valid (*e.g.*, that radio-loud and radio-quiet QSOs are more fundamentally associated).

In order to examine the question of whether the distinction between the radio-loud and radio-quiet families is mainly a result of the extended radio emission, we plotted in Fig. 3 the 5 GHz core radio luminosity against the [OIII] line luminosity. As we can see from the figure, the gap between the radio-loud and radio-quiet groups is much less pronounced in this case (although instrumental effects introduce uncertainties; see also Nelson & Whittle 1996 and Sadler *et. al.* 1995), but the two groups are still discernible. Interestingly, most of the “intermediate” sources of Fig. 1 become essentially indistinguishable from the radio-loud sources in Fig. 3. This may indicate a close relation between the intermediate sources and the radio louds. A linear fit to the core radio luminosity of the radio-louds gives

$$\log(L_{core}) = (0.78 \pm 0.07) \log(L_{[\text{OIII}]}) - (3.3 \pm 1.1) \quad , \quad (2)$$

where L_{core} is the core radio luminosity (at 5 GHz) in Watts Hz⁻¹ Sr⁻¹.

In order to further clarify the properties of the [OIII] emission, we plot in Fig. 4 the x-ray luminosity in the 2–10 keV band as a function of the [OIII] luminosity. As can be seen from the figure, a clear positive correlation exists, and a linear fit gives

$$\log(L_{HX}) = (1.01 \pm 0.08) \log(L_{[\text{OIII}]}) + (8.6 \pm 0.7) \quad , \quad (3)$$

where L_{HX} is the x-ray luminosity (in the 2–10 keV range) in erg s^{-1} . Individual fits to the radio-loud (plus intermediate) sample and the radio-quiet sample give slopes of 0.89 ± 0.19 and 0.95 ± 0.10 respectively.

It is important to note right away that the radio-louds and radio-quiet share the same L_{HX} – $L_{[OIII]}$ relation, implying probably that the same physical process relates these quantities in the two families (we will return to this point later).

In order to examine the potential effects of the environment, we also plotted the data of Fig. 1 distinguishing among the different types of host galaxies (in cases in which the latter have been identified). This is presented in Fig. 5. This figure confirms that *all* the radio louds are elliptical or S0 galaxies, while almost all of the spirals are radio quiet. It is interesting to note though that some of the “intermediate” objects are spirals. We should note, however, that quite a few of the morphologies are ambiguous (in particular the distinction between ellipticals and S0s) and therefore caution should be exercised in attempts to draw conclusions on the basis of morphology.

4. DISCUSSION

We have found that over a very wide range in luminosities, AGNs separate into two classes of objects, radio-loud and radio-quiet, and that the two classes obey two parallel relations between their radio and [OIII] luminosities, of the form

$$L_{5\text{ GHz}} \sim L_{[OIII]}^\beta \quad , \quad (4)$$

with $\beta \sim 0.5$ (Fig. 1 and eq. 1). At this point we need to consider whether the observed relationships are true correlations or whether selection effects can be dominating what we are seeing. First, we need to ask, are there really two distinct classes of radio-quiet and radio-loud types of AGN or is the apparent gap region merely an artifact of the selection

process? In particular, many, though not all, of the radio loud objects come from radio flux density selected samples and many, though not all, of the radio quiet objects come from optically selected samples.

We do not think that selection effects are responsible for the apparent population of the $L_{radio} - L_{[OIII]}$ plane for the following reasons: (i) radio flux density selected samples always include objects of low radio luminosity at low redshift and of progressively higher and higher radio luminosity with redshift. For example, the 3CR cut off in radio flux is about 9 Jy at 178 MHz (Bennett 1962); if we take the spectral index as 0.75 (which is a typical value for AGNs), then the extrapolated radio flux at 5 GHz is 0.74 Jy. This corresponds to $L_{5GHz} \sim 2.3 \times 10^{21} W/Hz/Sr$ at $z=0.003$ and $L_{5GHz} \sim 2.56 \times 10^{22} W/Hz/Sr$ at $z=0.01$. These values lie within the radio-quiet group in our classification (Fig. 1). Actually, we do find sources from the 3CR catalogue which are indeed radio-quiet (3C71 for example). Likewise, purely optically selected samples of AGN (e.g., Padovani 1993; Miller *et. al.* 1990 and Kellermann *et. al.* 1989) also show the radio-quiet-radio-loud dichotomy, with roughly 1 in 10 of optically selected quasars falling into the radio loud category. (ii) Perhaps more importantly, the apparent dichotomy in properties we have found is not a dichotomy of either L_{radio} or $L_{[OIII]}$, but the *ratio* of these two quantities. It is clear that selection effects can cause us to find sources with high, on average, radio luminosity when we select radio flux density limited samples; however, there is no a priori reason why such samples should show a limited and specific ratio of radio to line luminosity. The absence of identified sources with high radio luminosity and low line luminosity in radio flux density selected samples has been known for years (e.g., Baum and Heckman, 1989); sources with high radio luminosity invariably have high accompanying line luminosities. The real surprise is then that the *converse* does not also appear to be true. That is, if one selects AGN of high line luminosity at any given redshift, one finds two distinct classes of objects; those with high radio luminosity and those without. Said in a different way, there are sources with very

high line luminosity which do not have accompanying very high radio luminosity. This is the radio-quiet radio-loud dichotomy that has been known for many years (e.g., Antonucci 1993 and references therein); and the fundamental paradox: the nuclei of active galaxies can produce copious amounts of line luminosity (and UV through X-ray luminosity) without producing large amounts of radio luminosity, however the nuclei of active galaxies cannot produce large amounts of radio luminosity without producing concomitant large amounts of line and UV/X-ray luminosity.

4.1. The Physical Origin Of The $L_{radio} - L_{[OIII]}$ Relation

We will now attempt to understand the origin of this relation in terms of the physical processes involved.

There exists strong observational evidence that suggests that $L_{[OIII]}$ is one of the best orientation independent measures of the intrinsic luminosity of the nuclei of AGNs (e.g., Miller *et. al.* 1992; Jackson & Browne 1991; Mulchaey *et. al.* 1994). This fact, in combination with the data presented in Fig. 4, suggests that $L_{[OIII]}$ is proportional to the accretion rate through the accretion disk, \dot{M}_{acc} . We will therefore assume that $L_{[OIII]}$ is proportional to \dot{M}_{acc} , $L_{[OIII]} \propto \dot{M}_{acc}$.

We will now attempt to obtain a general relation between the accretion rate through the disk and the mass flux into the jet, \dot{M}_j (see e.g., Pringle 1993; Tout & Pringle 1996; Livio 1997).

To this goal, we first note that the most promising models for jet acceleration and collimation involve an accretion disk that is threaded by a large scale, vertical magnetic field (e.g., Blandford & Payne 1982; Königl 1989; and see Livio 1997 for a review). We will now make the following simple assumptions: (i) The accretion disk is largely a standard

(geometrically thin), Shakura-Sunyaev (1973) disk. (ii) The jet velocity, V_j , is of the order of the Keplerian velocity in the inner disk. (iii) The vertical magnetic field component is of the order of the azimuthal one, $B_z \sim B_\phi$. A detailed justification of these assumptions can be found in Livio (1999) and references therein. Realizing that the back pressure from the jet on the disk is given by $P_{jet} \sim \dot{M}_j V_j / R^2$, where R is the radius from which the jet originates, and using assumptions (i)–(iii) above, we obtain

$$\frac{B_z^2 / 8\pi}{P_g} \sim \frac{\dot{M}_j}{\dot{M}_{acc}} \frac{H}{R} \alpha . \quad (5)$$

Here P_g is the gas pressure, H is the disk half-thickness and α is the Shakura-Sunyaev (1973) viscosity parameter. If we assume in addition that the disk viscosity is generated by a dynamo, which in turn is powered by MHD turbulence (*e.g.*, Hawley, Gammie & Balbus 1995; Stone *et al.* 1996; Brandenburg *et al.* 1995), then $\alpha \sim B_D^2 / (4\pi P_g)$, where B_D is the magnetic field in the disk. Substituting this into eq. (5) gives

$$\frac{B_z}{B_D} \sim \left[\frac{\dot{M}_j}{\dot{M}_{acc}} \frac{H}{R} \right]^{1/2} . \quad (6)$$

An independent relation between B_z and B_D can be obtained if we make an assumption about the origin of the large-scale vertical field. In principle, such a field can either be advected inwards by the accreting matter (*e.g.*, Blandford & Payne 1982; Königl 1989; Pelletier & Pudritz 1992), or it can be generated locally by the same dynamo processes which generate the disk viscosity (Tout & Pringle 1996). If we assume the latter to be true, then the large scale field may be obtained through the reconnections of magnetic loops (leading to an inverse cascade process) which have a length distribution of the form $n(\ell) \sim \ell^{-\delta}$. In such a case, it can be easily shown that (Tout & Pringle 1996; Livio 1997)

$$\frac{B_z}{B_D} \sim \left(\frac{H}{R} \right)^{\delta-1} . \quad (7)$$

Combining eqs. (6) and (7) we obtain

$$\frac{\dot{M}_j}{\dot{M}_{acc}} \sim \left(\frac{H}{R} \right)^{2\delta-3} . \quad (8)$$

Observations of accretion disks, jets and outflows in young stellar objects, supersoft x-ray sources and cataclysmic variables and theoretical models suggest that δ is in the range 1.7–3.4 (Livio 1997; Tout & Pringle 1996). Therefore, assuming that the jet formation mechanism is similar in all the classes of objects which produce jets, and noting that H/R is approximately constant in standard disks (Shakura & Sunyaev 1973), we find that \dot{M}_j is roughly proportional to \dot{M}_{acc} , $\dot{M}_j \propto \dot{M}_{acc}$.

The final ingredient that is needed to explain the relation obtained in Fig. 1 is a relation between $L_{5\text{ GHz}}$ and \dot{M}_j . Since we have shown that $L_{[OIII]} \propto \dot{M}_{acc}$, and that $\dot{M}_j \propto \dot{M}_{acc}$, it is clear that the dependence observed in Fig. 1 (and in Rawlings 1994) would be obtained if $L_{5\text{ GHz}} \propto \dot{M}_j^\beta$, with $\beta \sim 0.5 - 1.0$. Observations of individual Galactic jets in systems containing black hole accretors (e.g., Hjellming & Rupen 1995; Mirabel & Rodriguez 1994; Tavani *et. al.* 1996) indeed suggest that the radio luminosity is proportional to some power (of order unity) of the mass flow rate into the jet. Simple models of radio emission from jets also predict radio luminosities which are roughly proportional to the mass flux into the jet (with the constant of proportionality depending on some power of the magnetic field strength and on the age of the source, *e.g.*, Bicknell, Dopita & O’Dea 1997). We therefore conclude that the general correlation in Fig. 1 is entirely consistent with a model in which jets are formed by accretion disks (around supermassive black holes) which are threaded by a vertical magnetic field (e.g., Blandford & Payne 1982; Königl 1989; Ostriker 1997; Matsumoto *et. al.* 1996; and see Livio 1997 for a review).

A question that needs to be asked at this point is: can there be important selection effects which are skewing the slope of the $L_{5\text{GHz}} - L_{[OIII]}$ correlation to be less than unity? This could occur, most naturally, if we were missing a class of high radio luminosity, high [OIII] luminosity objects or if we have systematically underestimated the line luminosity of the high luminosity objects. However, there is no evidence that this is the case. A fit

to the slope for only $z \geq 0.2$ radio-loud sources indicates, if anything, a slightly flatter slope (0.37 ± 0.12) than that found either at low ($z \leq 0.2$) redshifts or taking the sample as a whole (0.61 ± 0.07), though the differences are not statistically significant. Similarly, the slope of the radio-quiet class is more dominated by low redshift objects, but shows no evidence for a change for redshifts less than (slope 0.44 ± 0.07) or greater than 0.2 (slope 0.45 ± 0.55).

It is important to note that the fact that the $L_{5\text{ GHz}} - L_{[\text{OIII}]}$ relation *has almost the same slope* for both the radio-quiet and radio-loud AGNs probably indicates that the jet formation mechanism is the same in both of these subclasses.

4.2. The Black Hole Mass

Another consequence of Fig. 1 that should be pointed out is the following (see also Livio 1997). The mass of the central black hole determines the Eddington luminosity, and therefore the maximum accretion rate which the system can sustain (this translates into: how far to the right, in Fig. 1, the system can be found). Hence, we can expect that the AGNs containing the most massive black holes will occupy the upper right corner of the distribution for each subclass (radio-loud and radio-quiet). Interestingly, we find that the distribution of the radio-louds extends to somewhat larger values of $L_{[\text{OIII}]}$ (larger \dot{M}_{acc}). In order to further examine the implications of this fact, we show in Fig. 6 the distribution of the sources with respect to their redshifts. We find that the sources at low redshifts ($z \leq 0.2$) exhibit the same range in \dot{M}_{acc} ($L_{[\text{OIII}]}$) in both radio-louds and radio-quiet, but that the radio-loud sources at higher redshifts extend to higher values of \dot{M}_{acc} . Therefore, if the Eddington luminosity is indeed the limiting factor, then this finding can be regarded as suggestive that the maximum mass of the black holes found in radio-louds is higher than that in radio-quiet. This result would be consistent with the fact that the measured black hole masses appear to correlate with the bulge luminosities (Kormendy & Richstone 1995).

4.3. The Distinction Between Radio-Louds And Radio-Quiets

A more difficult and long standing question is what distinguishes the upper group (radio-louds) from the lower one (radio-quiets). Recent discussions of this problem can be found, for example, in Blandford & Levinson (1995), Fabian & Rees (1995), Wilson (1996) and Livio (1997).

Generally, explanations for the existence of these two classes fall into two different categories: (i) the ones that assume that the central engines in radio-louds and radio-quiets are the same, but that either the formation or the propagation of powerful jets is somehow prohibited in radio-quiets by some external circumstances. (ii) Ones in which it is assumed that only the central engines of the radio-louds can produce truly *powerful* jets.

In recent work, Livio (1997, 1999) examined the formation of jets in *all* the classes of astrophysical objects which are observed to produce jets. On the basis of the assumption that the jet formation mechanism is *the same* in all the classes of objects, Livio has shown that the following *conjecture* is consistent with all the available observational data: the formation of *powerful* jets requires in addition to an accretion disk threaded by a vertical field, an additional energy/wind source like a corona or a source associated with the central object. More recently, Ogilvie & Livio (1998) solved for the local vertical structure of an accretion disk threaded by a poloidal magnetic field. By analyzing the dynamics of the transonic outflow in the disk corona, they showed that a certain potential difference must be overcome even when the inclination angle between the magnetic field and the vertical to the disk surface is larger than 30° . Thus, the launching of an outflow from an accretion disk indeed requires a hot corona or access to an additional source of energy, in accordance with Livio's above conjecture. Livio went on to attempt to identify the extra energy/wind source for every jet-producing class. In the case of black hole accretors, the general impression has been that this source may be the black hole spin (since rotational energy can be

extracted, e.g., by the Blandford & Znajek (1977) mechanism). Observations suggesting that the spins of the two jet-producing Galactic black holes (GRS 1915+105 and GRO J1655-40) are high ($a_* = 0.998$ and 0.93 respectively, where a_* is the dimensionless specific angular momentum), while those of other stellar-mass black holes (which do not have jets) are very low ($a_* \sim 0$; Zhang, Cui & Chen 1997) seemed consistent with this impression (although the spin determinations are rather uncertain). However, more recently, Ghosh & Abramowicz (1997), Livio, Ogilvie & Pringle (1999), and Li (1999) have shown that the electromagnetic output from the inner disk is generally expected to dominate over that from the hole. Consequently, the spin of the hole may not be the “extra” energy source in Livio’s conjecture. Rather, the role of the “wind” from the central source in Livio’s conjecture may be played by gas pressure of the hot atmosphere in ellipticals, as suggested by Fabian & Rees (1995). The latter possibility may be supported by the fact that Fig. 5 shows that the high $L_{5\text{ GHz}}$ group contains quite a few S0 galaxies (but no spirals), in which the central environments are generally similar to those in ellipticals.

5. SUMMARY AND CONCLUSIONS

On the basis of the data collected in the present work and the discussion in §4, we can draw the following (tentative) conclusions: (1) Both radio-quiet and radio-loud AGNs obey a linear $\log L_{5\text{ GHz}} - \log L_{[OIII]}$ relation, with a nearly identical slope (but with a shift towards higher radio power for the radio-louds, by a factor $\sim 10^3 - 10^4$; see also Rawlings 1994). (2) The radio-louds and radio-quietes share the *same* linear correlation between $\log L_x$ and $\log L_{[OIII]}$ (where L_x is the X-ray luminosity in the 2-10 keV range). (3) Consistently with previous studies, we find that radio-loud AGNs are found only in elliptical and S0 galaxies (although the distinction between S0 and elliptical is often ambiguous), while radio-quietes are mostly spirals and S0s. (4) The observationally determined $L_{5\text{ GHz}} - L_{[OIII]}$

correlation is consistent with a model in which the radio-emitting jets are formed by an accretion disk which is threaded by a vertical magnetic field. (5) It is still not entirely clear whether the distinction between radio-louds and radio-quietes is a consequence of differences in the central engines of these two classes or whether it merely reflects differences in the environments.

Acknowledgments: ML acknowledges support from NASA Grant NAG5-6857. This work has been supported in part by the Director's Discretionary Research Fund at STScI. We acknowledge useful discussions with Andrew Wilson.

REFERENCES

- Antonucci, R., 1993, *ARA&A*, 31, 473
- Baum, S.A., and Heckman, T., 1989, *ApJ*, 336, 681
- Bennett, A.S., 1962, *MmRAS*, 68, 163
- Bicay, M.D., Kojoian, G., Seal, J., Dickinson, D.F., and Malkan, M.A., 1995, *ApJS*, 98, 369
- Bicknell, G.V., Dopita, M.A., and O’Dea, C.P., 1997, *ApJ*, 485, 112
- Blandford, R.D., and Levinson, A., 1995, *ApJ*, 441, 79
- Blandford, R.D., and Payne, D.G., 1982, *MNRAS*, 199, 883
- Blandford, R.D., and Znajek, R.L., 1977, *MNRAS*, 179, 433
- Blandford, R.D., 1990, in *Active Galactic Nuclei*, ed. T.J.L. Courvoisier & M. Mayor, Saas-Fee Advanced Course 20, (Springer), p. 161
- Boroson, T., and Green, R., 1992, *ApJS*, 80, 109
- Braatz, J.A., Wilson, A.S., and Henkel, C., 1997, *ApJS*, 110, 321
- Brandenburg, A., Norlund, A., and Stein, R.F., 1995, *ApJ*, 446, 741
- Brinkmann, W., Siebert, I., and Boller, Th., 1994, *A&A*, 281, 355
- Brinkmann, W., Siebert, J., Reich, W., Furst, E., Reich, P., Voges, W., Trumper, J., and Wielebinski, R., 1996, *A&AS*, 109, 147
- Brotherton, M.S., 1996, *ApJS*, 102, 1
- Ceballos, M.T., and Barcons, X., 1996, *MNRAS*, 282, 493
- Ceca, R., Palumbo, G., Persic, M., Boldt, E., Zotti, G., and Marshall, E., 1990, *ApJS*, 72, 471
- Condon, J.J., Frayer, D.T., and Broderick, J.J., 1991, *AJ*, 101, 362

- Dahari, O., and De Robertis, M.M., 1988, *ApJS*, 67, 249
- Fabbiano, G., Miller, L., Trinchieri, G., Longair, M., and Elvis, M., 1984, *ApJ*, 227, 115
- Fabian, A.C., and Rees, M.J., 1995, *MNRAS*, 277, L55
- Feretti, L., Giovannini, G., Gregorini, L., Parma, P., and Zamorani, G., 1984, *A&A*, 139, 55
- Gelderman, R., and Whittle, M., 1994, *ApJS*, 91, 491
- Ghosh, P., and Abramowicz, M.A., 1997, *MNRAS*, 292, 887
- Giovannini, G., Feretti, L., Gregorini, L., and Parma, P., 1988, *AA*, 199, 73
- Gregory, P.C., and Condon, J.J., 1991, *ApJS*, 75, 1011
- Griffith, M.R., Wright, A.E., Burke, B.F., and Ekers, R.D., 1994, *ApJS*, 90, 179
- Hawley, J.F., Gammie, J.F., and Balbus, S.A., 1995, *ApJ*, 440, 743
- Heckman, T., O’Dea, C., Baum, A.S., and Laurikainen, E., 1994, *ApJ*, 428, 65
- Herbig, T., and Readhead, A.S., 1992, *ApJS*, 81, 83
- Hjellming, R.M., and Rupen, M.P., 1995, *Nature*, 375, 464
- Ho, L.C., Filippenko, A.V., and Sargent, W.L.W., 1993, *ApJ*, 417, 63
- Jackson, N., and Browne, W.A., 1990, *Nature*, 343, 43
- Jackson, N., and Browne, W.A., 1991, *MNRAS*, 250, 414
- Kaastra, J.S., Kunueda, H., and Awaki, H., 1991, *A&A*, 242, 27
- Kellermann, K.I., Sramek, R., Schmidt, M., Shaffer, D.B., Green, R., 1989, *AJ*, 98, 1195
- Kojoian, G., Tovmasian, K.H.M., Dickinson, D.F., and Dinger, A.S.C., 1980, *AJ*, 85, 1462
- Kormendy, J., and Richstone, D., 1995, *ARA&A*, 33, 581
- Königl, A., 1989, *ApJ*, 342, 208
- Koski, A.T., 1978, *ApJ*, 223, 56

- Kuhr, H., Pauliny-Toth, I.I.K., Witzel, A., and Schmidt, J., 1981, *AJ*, 86, 854
- Laing, R.A., Riley, J.M., and Longair, M.S., 1983, *MNRAS*, 204, 151
- Li, L.-X., 1999, astro-ph/9902352
- Lipovetsky, V.A., Neizvestny, S.I., and Neizvestnara, O.M., 1988, *Comm. SAO (USSR)*, 55,
A Catalogue of Seyfert Galaxies.
- Livio, M., 1997, in IAU Colloquium, 163, *Accretion Phenomena and Related Outflows*, ed.
D.T. Wickramasinghe, L. Ferrario & G.V. Bicknell (San Francisco: ASP Vol. 121),
845
- Livio, M., 1999, *Physics Reports*, 311, 225
- Livio, M., Ogilvie, G.I., and Pringle, J.E., 1999, *ApJ*, 512, 100
- Matsumoto, R., Uchida, Y., Hirose, S., Shibata, K., Hayashi, M.R., Ferrari, A., Bodo, G.,
and Norman, C., 1996, *ApJ*, 461, 115
- Miller, L., Peacock, J.A., and Mead, A.R.G., 1990, *MNRAS*, 244, 207
- Miller, P., Rawlings, S., Saunders, R., and Eales, S., 1992, *MNRAS*, 254, 93
- Miller, P., Rawlings, S., and Saunders, R., 1993, *MNRAS*, 263, 425
- Mirabel, I.F., and Rodriguez, L.F., 1994, *Nature*, 371, 46
- Morganti, R., Killeen, N.E.B., and Tadhunter, C.N., 1993, *MNRAS*, 263, 1023
- Mulchaey, J.S., Koratkar, A., Ward, M.J., Wilson, A.S., Whittle, M., Antonucci, R.J.,
Kinney, A.L., and Hurt, T., 1994, *ApJ*, 436, 586
- Nelson, C.H., and Whittle, M., 1996, *ApJ*, 465, 96
- Ogilvie, G.I., and Livio, M., 1998, *ApJ*, 499, 329
- Ostriker, E.C., 1997, in IAU Colloquium, 163, *Accretion Phenomena and Related Outflows*,
ed. D.T. Wickramasinghe, L. Ferrario & G.V. Bicknell (San Francisco: ASP Vol.

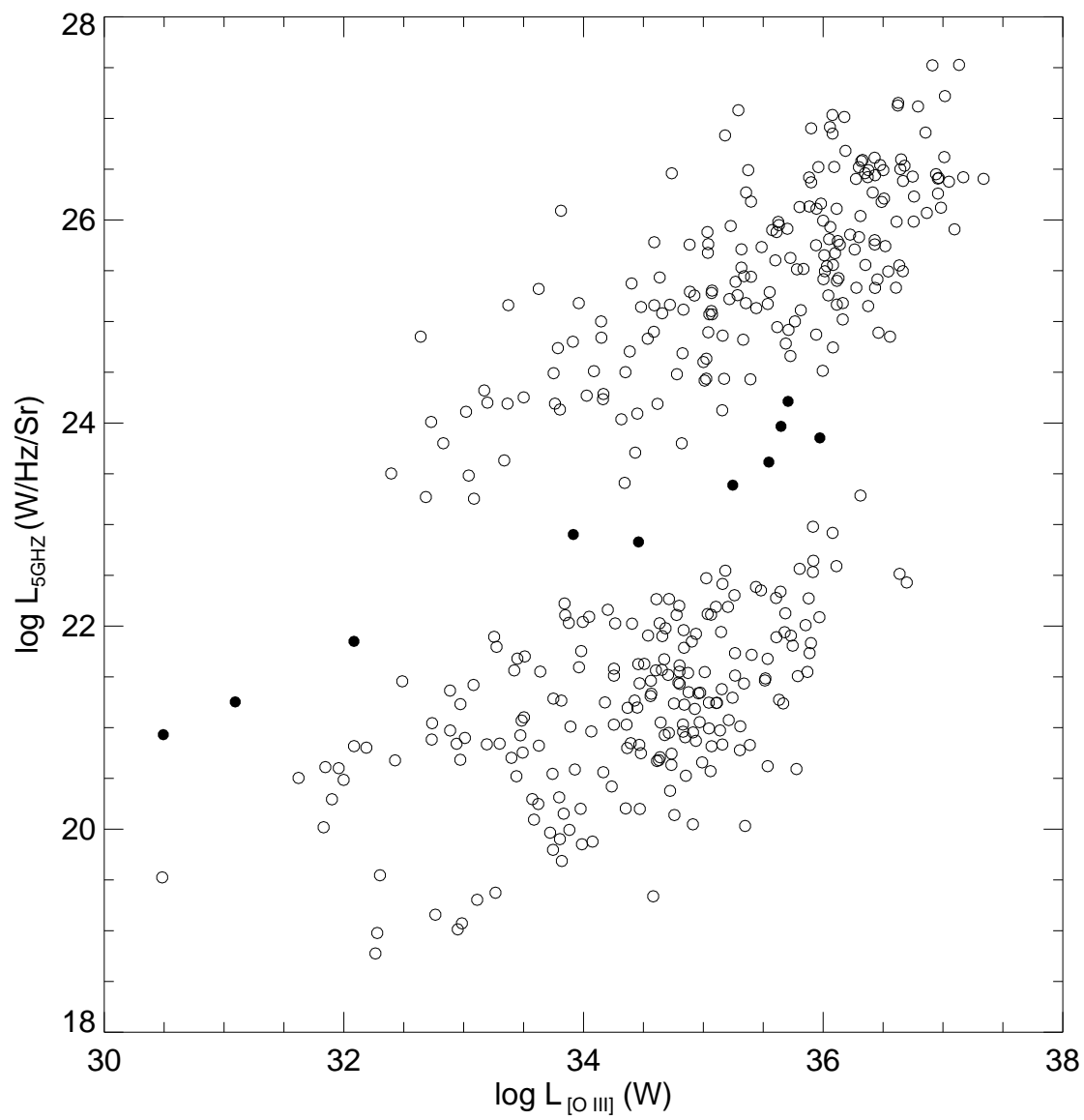
- 121), 439
- Padovani, P., 1993, MNRAS, 263, 461
- Padovani, P., and Giommi, P., 1995, MNRAS, 277, 1477
- Pauliny-Toth, I.I.K., and Kellermann, K.I., 1968, AJ, 73, 953
- Pauliny-Toth, I.I.K., and Kellermann, K.I., 1972, AJ, 77, 797 (1972a)
- Pauliny-Toth, I.I.K., Kellermann, K.I., Davis, M.M., Fomalont, E.B., and Shaffer, D.B., 1972, AJ, 77, 265 (1972b)
- Pauliny-Toth, I.I.K., Witzel, A., Preuss, E., *et. al.*, 1978, AJ, 83, 451
- Pelletier, G., and Pudritz, R., 1992, ApJ, 394, 117
- Perlman, E.S., Stocke, J.T., Schachter, J.F., Elvis, M., and Ellingson, E., *et. al.*, 1996, ApJS, 104, 251
- Polletta, M., Bassani, L., Malaguti, G., Palumbo, G.G.C., and Caroli, E., 1996, ApJS, 106, 399
- Pounds, K.A., 1990, MNRAS, 242, L20
- Pringle, J., 1993, in *Astrophysical Jets*, ed. D. Burgarella, M. Livio & C.P. O’Dea (Cambridge: Cambridge University Press), p. 1
- Rawlings, S., Saunders, R., Eales, S.A., and Mackeny, C.D., 1989, MNRAS, 240, 701
- Rawlings, S., and Saunders, R., 1991, Nature, 349, 138
- Rawlings, S., 1994, in *The First Stromlo Symposium: The Physics of Active Galaxies*, ed. G. Bicknell, M. Dopita, & P. Quinn (ASP Conference Series, Vol 54), p. 253
- Rothschild, R.E., Mushotzky, R.F., Baity, W.A., Gruber, D.E., Matteson, J.L., and Peterson, L.E., 1983, ApJ, 269, 423
- Rush, B., Malkan, M., Fink, H., and Voges, W., 1996, ApJ, 471, 190

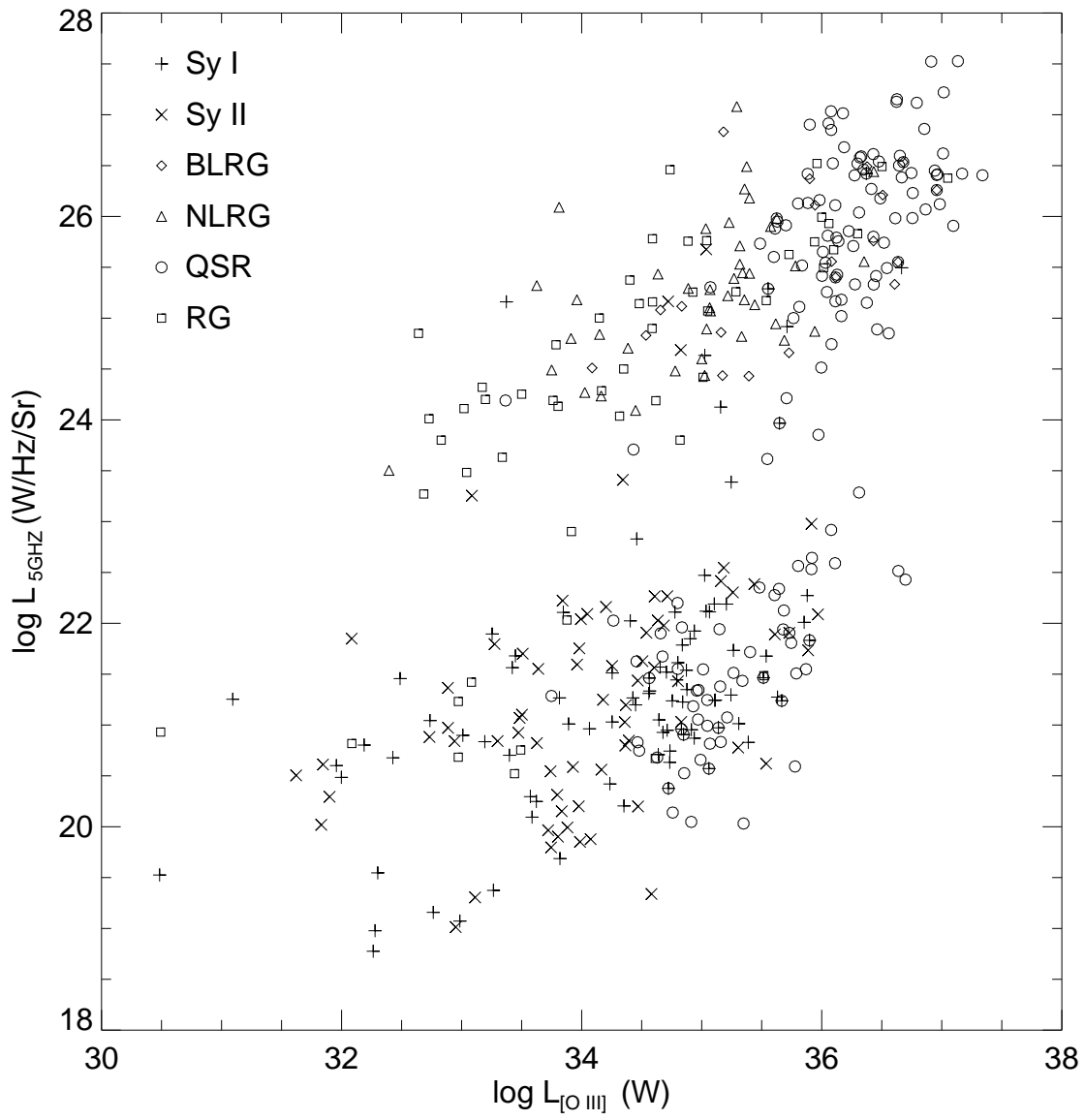
- Sadler, E.M., Slee, O.B., Reynolds, J.E., and Roy, A.L., 1995, MNRAS, 276, 1373
- Schmidt, M., and Green, R.F., 1983, ApJ, 269, 352
- Shakura, N.I., and Sunyaev, R.A., 1973, A&A, 24, 337
- Shimmins, A.J., Bolton, J.G., 1972, Aus JPAS, 23, 1
- Shimmins, A.J., Bolton, J.G., and Wall, J.V., 1975, Aus JPAS, 34, 63
- Siebert, J., Brinkmann, W., Morganti, R., Tadhunter, C.N., Danziger, I.J., Fosbury, R.A.E.,
and Di Serego Alighieri, S., 1996, MNRAS, 279, 1331
- Simpson, C., Ward, M., Clements, D.L., Rawlings, S., 1996, MNRAS, 281, 509
- Smith, H.E., and Spinrad, H., 1980, PASP, 92, 553
- Sramek, R.A., 1975, AJ, 80, 771
- Steiner, J.E., 1981, ApJ, 250, 469
- Stocke, J.T., Morris, S.L., Gioia, I.M., Maccacaro, T., Schild, R.E., and Wolter, A., 1990,
ApJ, 348, 141
- Stocke, J.T., Morris, S.L., Gioia, I.M., Maccacaro, T., Schild, R.E., Wolter, A., Flemingo,
T., and Henry, J.P., 1991, ApJS, 76, 813
- Stone, J., Hawley, J.F., Gammie, C.F., and Balbus, S.A., 1996, ApJ, 463, 656
- Tabara, H., and Inoue, M., 1980, A&AS, 39, 379
- Tadhunter, C.N., Morganti, R., Di Serego Alighieri, S., Fosbury, R.A.E., Danziger, I.J.,
1993, MNRAS, 263, 999
- Tavani, M., Fruchter, A., Zhang, S.N., Harmon, B.A., Hjellming, R.N., Rupen, M.P.,
Bailyn, C., and Livio, M., 1996, ApJ, 473, 103
- Tout, C., and Pringle, J.E., 1996, MNRAS, 281, 219
- Turner, M.J., William, D.R., Stewart, G.C. *et. al.*, 1989, xrbi.2.769

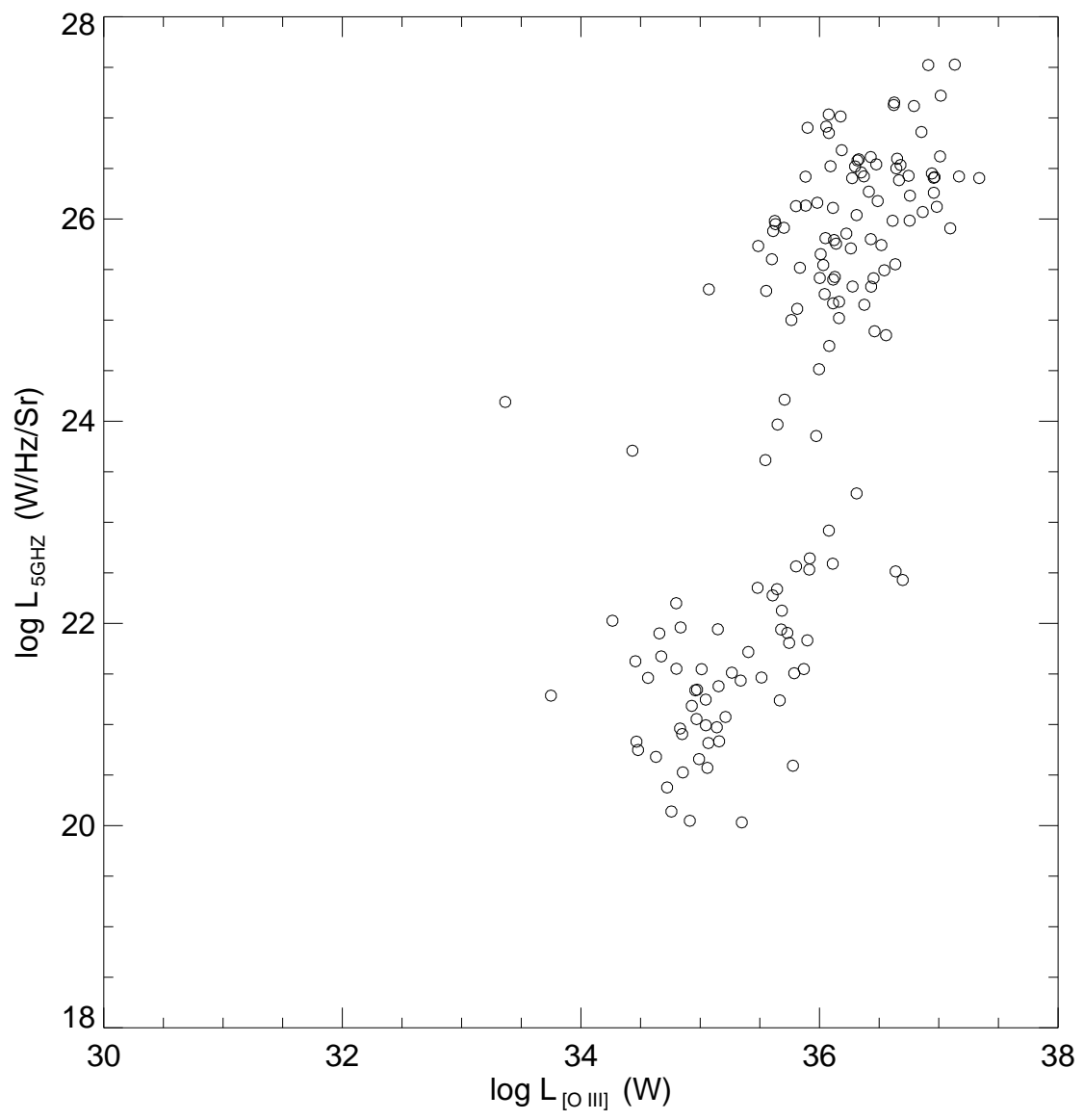
- Ulrich, M., and Meier, D.L., 1984, AJ, 89, 203
- Ulvestad, J.S., and Wilson, A.S., 1984, ApJ, 285, 439 (1984a)
- Ulvestad, J.S., Wilson, A.S., 1984, ApJ, 278, 544 (1984b)
- Ulvestad, J.S., and Wilson, A.S., 1989, ApJ, 343, 659
- Unger.S.W., Lawrence, A., Wilson, A.S., Elvis, M., and Wright, A.E., 1987, MNRAS, 228,
521
- Urry, C.M., and Padovani, P., 1995, PASP, 107, 803
- Veron-Cetty, M.P., and Veron, P., 1996, ESO Scientific Report, Quasars and Active Galactic
Nuclei (7th Ed.)
- Whittle, M., 1992, ApJS, 79, 49
- Wilson, A.S., 1996, in *Energy Transport in Radio Galaxies and Quasars*, ed. P. Hardee, A.
Bridle, & J. Zensus, (ASP Conference Series, Vol 100), p. 9
- Zhang, S.N., Cui, W., and Chen, W., 1997, ApJ, 482, 155
- Zirbel, E.L., and Baum, S.A., 1995, ApJ, 448, 521

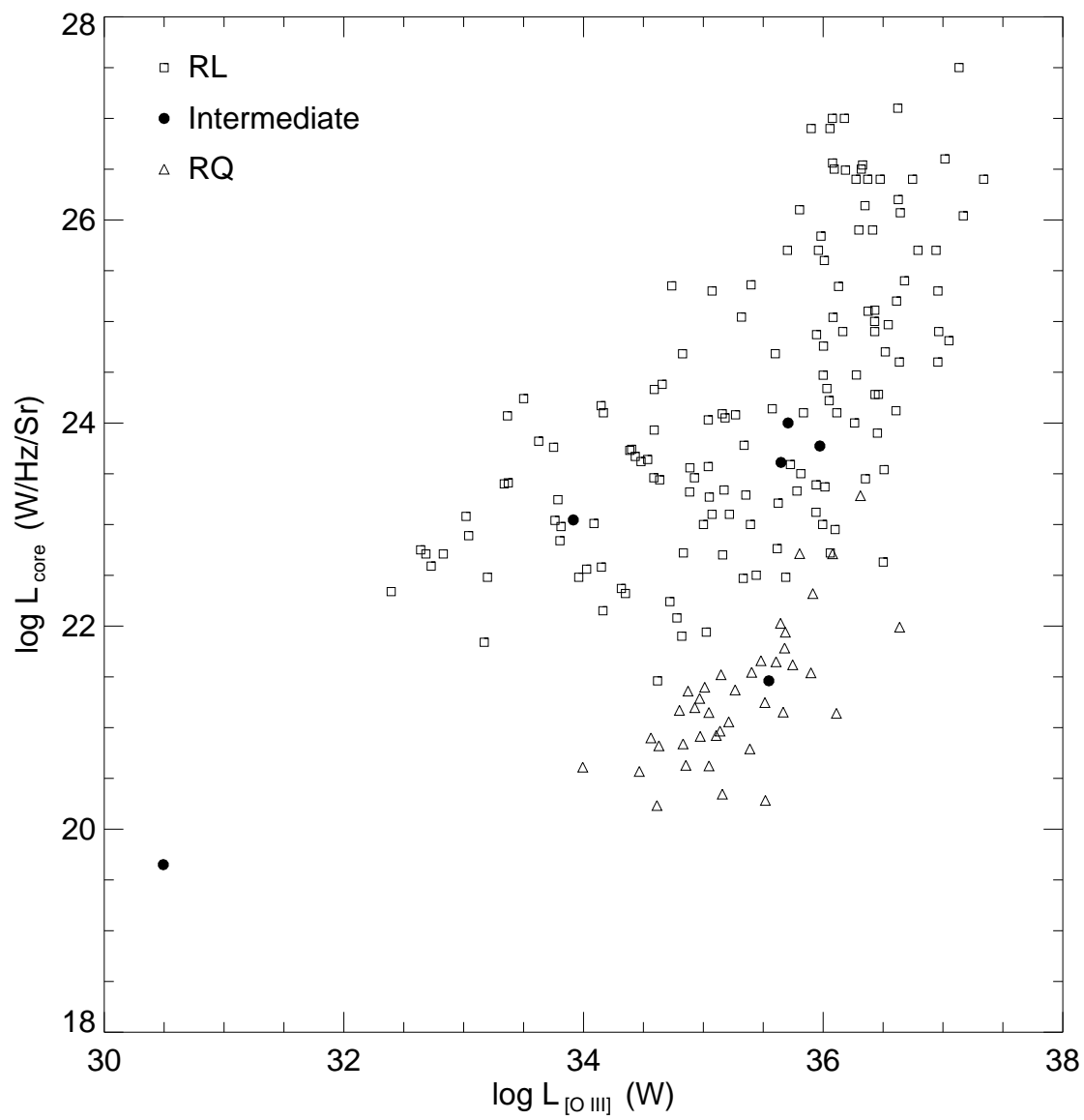
Figure Captions

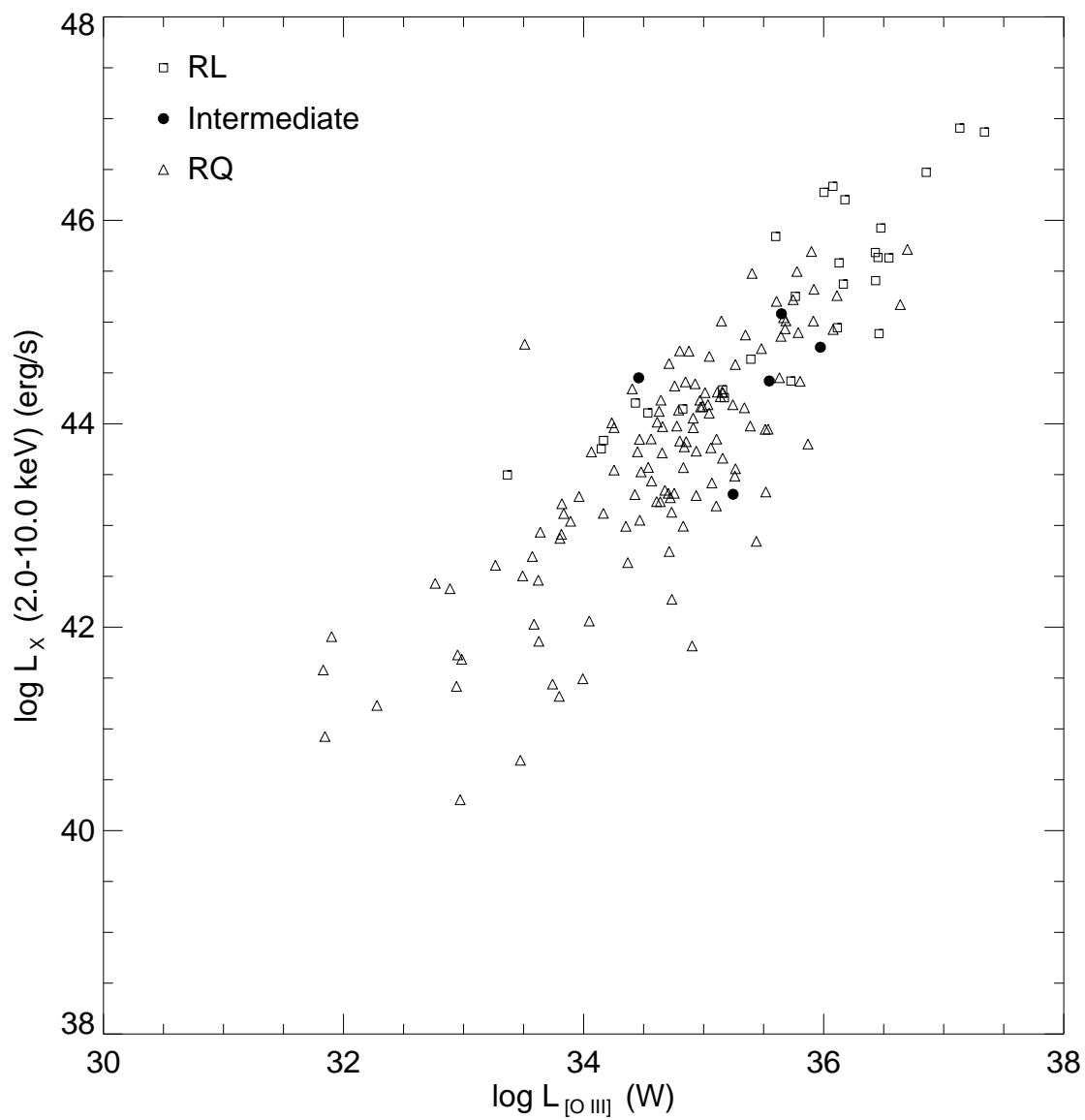
- Fig 1.** The total 5 GHz luminosity *vs.* the [OIII] 5007 line luminosity for our sample of AGNs. The filled circles represent the intermediate sources (see text).
- Fig 2a.** Same as Fig 1., with the types of the AGNs indicated.
- Fig 2b.** Same as Fig 1., but only the Quasars are presented.
- Fig 3.** The core 5 GHz luminosity *vs.* the [OIII] 5007 luminosity. Most of the objects presented here are radio-louds.
- Fig 4.** The hard X-ray luminosity (2 – 10 keV) *vs.* the [OIII] 5007 luminosity.
- Fig 5.** Same as Fig 1., with the morphological type of the host galaxies of the AGNs indicated. (Note that the symbols that appear as filled squares are actually filled circles reside in open squares, in case in which an ambiguity exists)
- Fig 6.** Same as Fig 1., with the redshift ranges indicated.

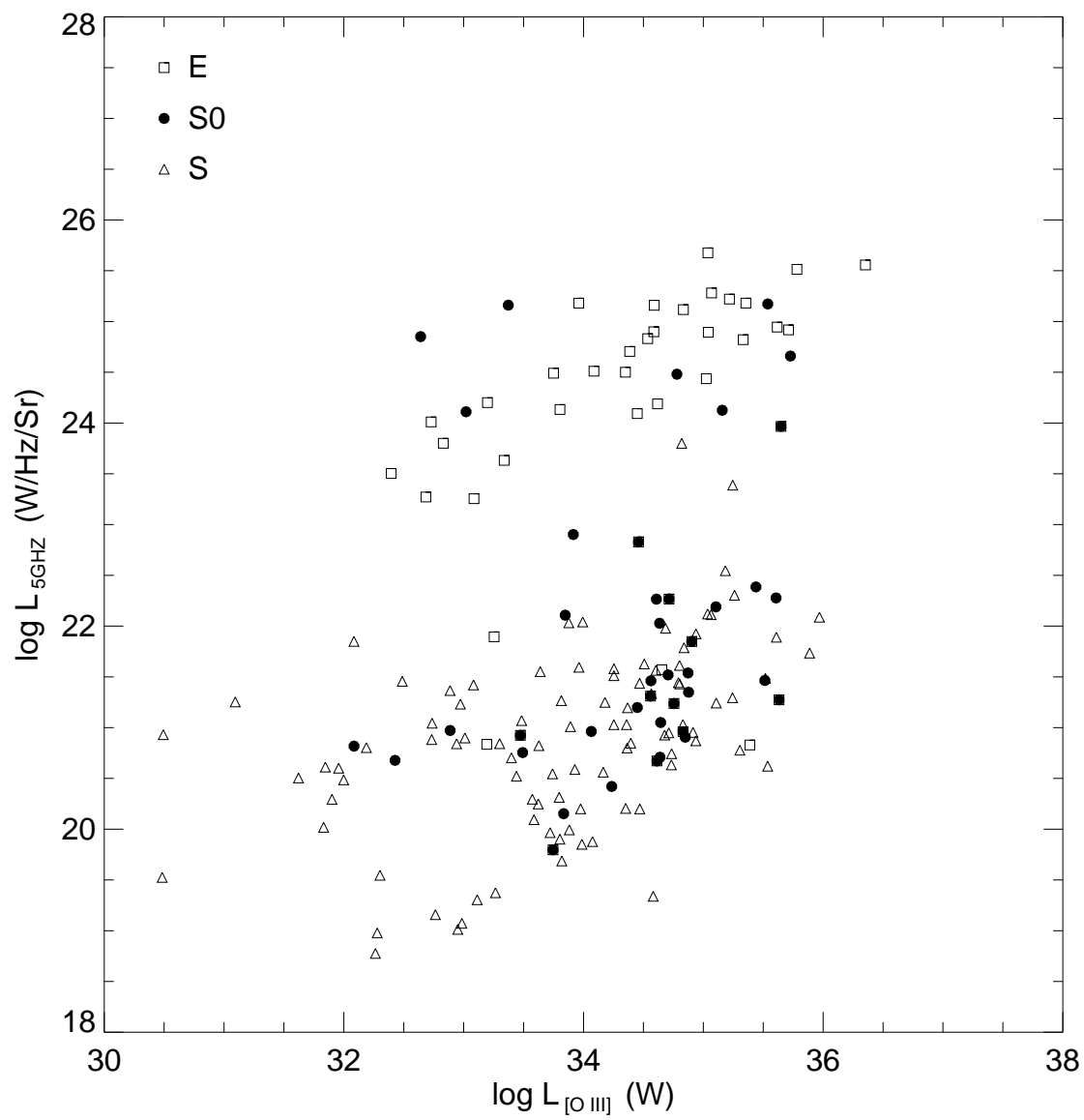












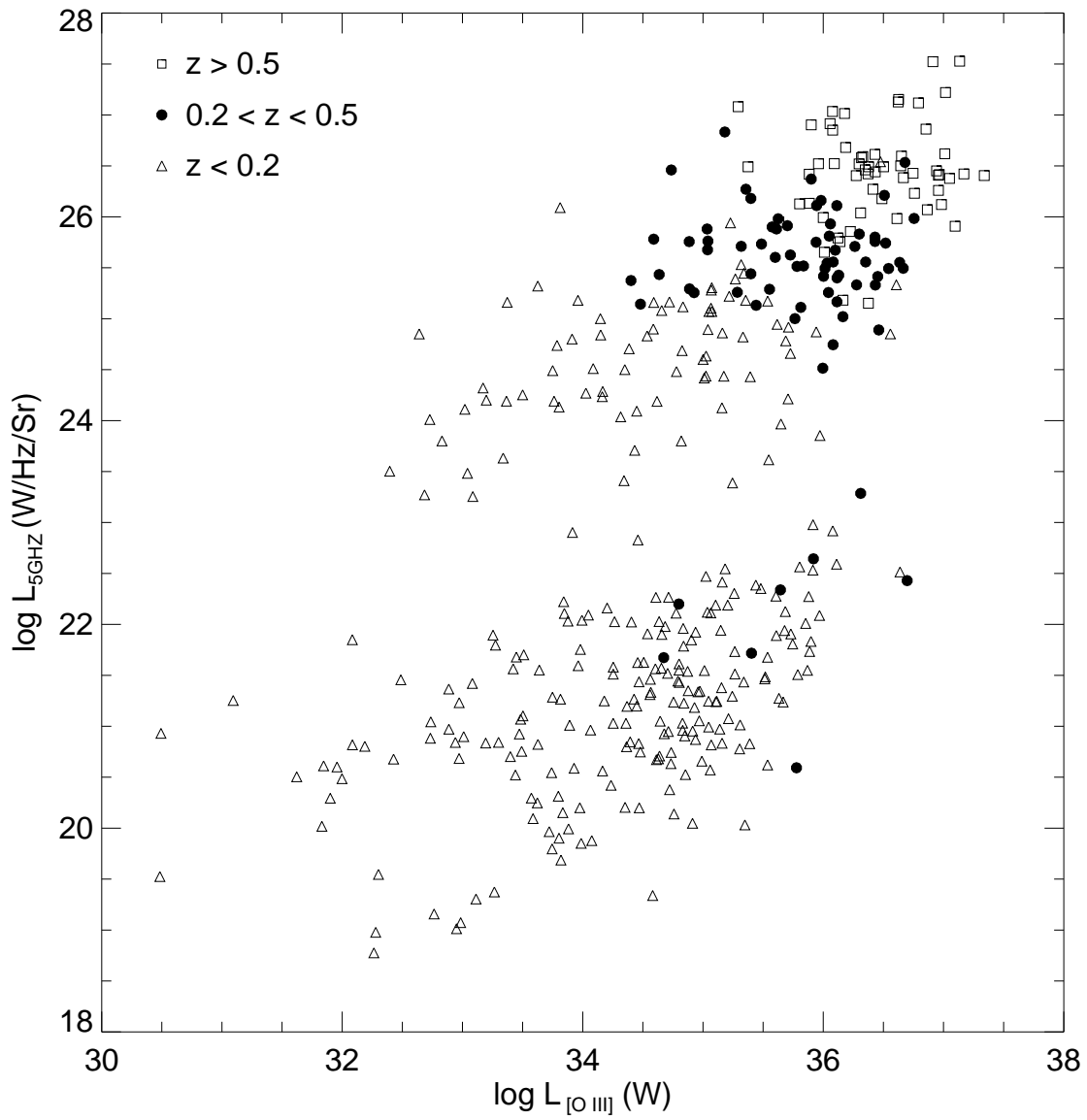


TABLE 1. AGN LIST

object (1)	name (2)	ID (3)	class (4)	morph (5)	z (6)	L_{oiii} (7a)	ref (7b)	P5 (8a)	ref (8b)	PC5 (9a)	ref (9b)	Lx (10a)	ref (10b)	Remark (11)
0000+21	Mrk 334	G	Sy1.8	Pec	0.0220	34.426	PBMP	21.266	PBMP			43.303	CPPB	Q
0003+15	PG 0003+15	Q			0.4499	36.543	BG	25.492	KSSS	24.968	KSSS	45.631	CPPB	L
0003+19	Mrk 335	Q	Sy1.0	E/S0	0.0258	34.830	W	20.960	KSSS	20.840	KSSS	43.569	CB	Q
0007+10	PG 0007+10	Q	Sy1.0	E/S0	0.0890	35.648	DR	23.967	KSSS	23.611	KSSS	45.081	CPPB	I
0007+25	NGC 0023	G		SB(s)a	0.0152	33.081	DR	21.420	KTDD					Q
0008-12	NGC 0034	G	Sy2.0	Pec	0.0198	33.274	PBMP	21.795	PBMP					Q
0023-26	PKS 0023-26	G	NLRG		0.3220	35.397	TMDF	26.180	MKT					L
0026+12	PG 0026+12	Q			0.1420	36.110	DR	22.590	KSSS	21.140	KSSS	45.260	CPPB	Q
0034-01	3C 15	G	NLRG	E	0.0730	33.750	TMDF	24.490	MKT	23.760	ZB			L
0035-02	3C 17	G	NLRG	N	0.2200	35.318	TMDF	25.710	MKT	25.043	MKT			L
0038+09	3C 18	G	NLRG		0.1880	35.268	TMDF	25.390	MKT	24.080	ZB			L
0039-44	PKS 0039-44	G			0.3459	36.299	TMDF	25.830	MKT					L
0042+10		Q			0.5830	36.164	JB1	25.181	BSRF					L
0043+03	PG 0043+03	Q			0.3840	34.798	BG	22.199	KSSS					Q
0043-42	PKS 0043-42	G	NLRG	E	0.1160	33.960	TMDF	25.180	MKT	22.480 [†]	ZB			L
0045-25	NGC 0253	G		Sc	0.0010	30.493	TMDF	20.930	MKT	19.650	ZB			I
0046+31	NGC 0262	G	Sy2.0	S0	0.0149	34.608	W	22.265	CFB			43.234	PBMP	Q
0049+17	PG 0049+17	Q	Sy1.0		0.0640	35.139	MRSE	20.972	KSSS	20.965	KSSS	44.266	CPPB	Q
0050+12	PG 0050+12	G	Sy1.0	S0	0.0610	34.872	DR	21.538	KSSS	21.359	KSSS			Q
0052+25	PG 0052+25	Q	Sy1.5		0.1550	35.898	MRSE	21.832	KSSS	21.539	KSSS	45.693	CB	Q
0055+30	NGC 0315	G		E	0.0173	32.684	HFS	23.271	CFB	22.710	ZB			L
0055-01	3C 29	G		E	0.0450	33.198	TMDF	24.200	MKT	22.480	ZB			L
0056-00	PHL 9234	Q			0.7170	36.650	JB1	26.596	BSRF					L
0105-16	3C 32	Q	NLRG		0.4000	35.625	TMDF	25.980	MKT	23.210 [†]	ZB			L
0106+13	3C 33	G	NLRG	E	0.0600	35.332	RSEM	24.820	HR	22.470				L
0106+72	3C 33.1	G			0.1810	35.049	JB2	25.070	HR	23.270	ZB			L
0107-03		Q	Sy2.0		0.0546	35.730	PBMP	21.906	PBMP					Q
0109-38	TOL 0109-383	G	Sy2.0	(R)SB0/a	0.0117	34.394	PBMP	20.846	PBMP					Q
0110+29	4C 29.02	Q			0.3630	36.043	JB1	25.257	BSRF					L
0111-15	Mrk 1152	G	Sy1.0	S/Pec	0.0527	34.711	W	20.948	ULWE			44.592	CB	Q

TABLE 1 ... CONTINUED

object	name	ID	class	morph	z	L_{oiii}	ref	P5	ref	PC5	ref	Lx	ref	Remark
(1)	(2)	(3)	(4)	(5)	(6)	(7a)	(7b)	(8a)	(8b)	(9a)	(9b)	(10a)	(10b)	(11)
0113+32	NGC 449	G	Sy2.0	(R)SB0/a	0.0167	34.604	DR	21.564	NED					Q
0115+02	3C 37	Q			0.6719	36.487	JB1	26.177	BSRF					L
0116+31	B2 0116+31				0.0590	33.500	GW	24.252	HR	24.240 [†]	ZB			L
0117-15	3C 38	G	NLRG		0.5650	36.432	TMDF	26.440	MKT					L
0118+03	3C 39	Q			0.7649	37.096	JB1	25.907	BSRF					L
0119+04	OC 033	Q			0.6370	35.803	JB1	26.127	BM	26.100	BM			L
0119+22	PG 0119+22	G		SB	0.0529	35.517	MRSE	21.484	KSSS	20.283	KSSS	43.329	CPPB	Q
0119-01	Mrk 1503	G	Sy1.5	SBa	0.0543	34.938	DR	21.923	NED			43.730	CPPB	Q
0121-35	NGC 526A	G	Sy1.5	S0	0.0192	34.638	W	20.708	PBMP			43.234	PBMP	Q
0122+31	Mrk 993	G	Sy1.9	Sa	0.0169	33.572	DR	20.295	NED			42.695	CPPB	Q
0125+28	3C 42	G			0.3950	34.885	RSEM	25.756	HR	23.320	ZB			L
0130+35	NGC 591	G	Sy2.0	(R)SB0/a	0.0151	34.364	W	20.799	UW2					Q
0131-36	NGC 612	G		S0	0.0300	33.019	TMDF	24.110	MKT	23.080	ZB			L
0132+37	3C 46	G			0.4370	36.014	RSEM	25.494	HR	23.370	ZB			L
0133+20	3C 47	Q			0.4250	36.518	JB1	25.742	BM	24.700	BM			L
0134+32	3C 48	Q	BLRG		0.3670	36.679	RSEM	26.533	BM	25.400	BM			L
0135-24	OC 259	Q			0.8309	36.746	JB1	26.427	BM	26.400	BM			L
0141+02	Mrk 573	G	Sy2.0	SAB0	0.0170	35.304	W	20.777	PBMP					Q
0152+06	UM 146	G	Sy1.9	SA(rs)b	0.0172	33.891	PBMP	21.010	PBMP			43.041	CPPB	Q
0157+00	PG 0157+00	Q			0.1640	36.078	MRSE	22.918	KSSS	22.712	KSSS	44.926	CPPB	Q
0157+02		G	Sy1.0	E/S0	0.0788	34.459	DR	22.828	NED			44.451	CPPB	I
0158-07	NGC 788	G	Sy2.0	SA0	0.0135	34.075	W	19.877	UW2					Q
0159-11	3C 57	Q			0.6690	36.644	TMDF	26.500	MKT	26.070	SBMT			L
0205+02			Sy1.0		0.1565	35.879	S1	22.273	NED					Q
0211-01	NGC 863	G	Sy1.5	SAa	0.0277	34.253	DR	21.029	UW3			43.962	CB	Q
0213-13	3C 62	G	NLRG	E	0.1480	35.355	TMDF	25.180	MKT	23.290	ZB			L
0221+27	3C 67	G	BLRG		0.3100	36.082	GW	25.556	HR	25.040	ZB			L
0232-09	NGC 985	G	Sy1.0	(R)Sa/Pec	0.0431	35.243	W	21.294	UW3			44.187	CB	Q
0235-19	PKS 0235-19	G			0.6200	36.501	TMDF	26.490	MKT	22.630 [†]	ZB			L
0238+06	Mrk 595	G	Sy1.0	E/S0	0.0259	34.903	W	21.847	NED			41.815	CPPB	Q

TABLE 1 ... CONTINUED

object (1)	name (2)	ID (3)	class (4)	morph (5)	z (6)	L_{oiii} (7a)	ref (7b)	P5 (8a)	ref (8b)	PC5 (9a)	ref (9b)	Lx (10a)	ref (10b)	Remark (11)
0238-08	NGC 1052	G	Sy3.0	E0	0.0051	33.253	DR	21.894	NED					Q
0240-00	3C 71	G	Sy2.0	(R)SA(r)a	0.0038	33.993	TMDF	22.040	HR	20.610	ZB	41.493	PBMP	Q
0252-00	NGC 1144	G	Sy2.0	(R)/Pec	0.0291	34.202	PBMP	22.160	PBMP					Q
0252-71	PKS 0252-71	G	NLRG		0.5660	35.374	TMDF	26.490	MKT					L
0256+36	Mrk 1066	G	Sy2.0	(R)SB(s)0	0.0120	34.178	W	21.248	UW2					Q
0258+35	NGC 1167	G		S0	0.0164	33.914	HFS	22.902	CFB	23.045	FGGP			I
0307+16	3C 79	G	NLRG	E	0.2560	36.352	RSEM	25.556	HR	23.450	ZB			L
0308-09	NGC 1241	G	Sy2.0	SB(r)b	0.0133	32.886	DR	21.365	NED					Q
0316+41	3C 84	G	Sy2.0	Pec	0.0175	34.826	PBMP	24.686	CFB	24.682		44.145	PBMP	L
0322-06	Mrk 609	G	Sy1.0	E/S0	0.0341	34.559	W	21.310	PBMP					Q
0325+02	3C 88	G		Pec/E	0.0300	32.829	TMDF	23.800	MKT	22.710	ZB			L
0328-03	Mrk 612	G	Sy2.0	(R)Sa	0.0201	34.507	W	21.627	PBMP					Q
0331-05	NGC 1358	G	Sy2.0	SB0a	0.0131	33.986	W	19.851	UW2					Q
0334-36	NGC 1386	G	Sy2.0	Sa	0.0046	33.881	W	19.993	UW1					Q
0336-01	CTA 26	Q			0.8520	36.056	JB1	26.914	BM	26.900	BM			L
0345+33	3C 93.1	G			0.2440	35.285	GW	25.259	PK1					L
0349-27	PKS 0349-27	G		E	0.0660	34.349	TMDF	24.500	MKT	22.320	ZB			L
0356+10	3C 98	G		E1	0.0310	34.617	RSEM	24.188	HR	21.460	ZB			L
0403-13	OF 105	Q			0.5709	36.318	JB1	26.579	BM	26.500	BM			L
0404+03	3C 105	G	NLRG		0.0890	34.149	TMDF	24.840	MKT	22.580	ZB			L
0405-12	OF 10904-1	Q			0.5740	37.169	TMDF	26.420	MKT	26.040	MKT			L
0409-75	PKS 0409-75	G	NLRG		0.6930	35.292	TMDF	27.080	MKT					L
0410+11	3C 109	G	BLRG	N	0.3060	36.430	RSEM	25.758	HR	25.110	ZB			L
0411+14	4C 14.11	G			0.2070	34.480	RSEM	25.142	HR	23.620	ZB			L
0412-08			Sy1.5		0.0383	35.308	S3	21.013	NED					Q
0414-06	3C 110	Q			0.7810	36.983	JB1	26.120	BM					L
0418-55	NGC 1566	G	Sy1.5	(R)Sb	0.0044	33.398	W	20.702	NED					Q
0430+05	3C 120	G	Sy1.0	S0?	0.0335	35.157	TMDF	24.125	CFB	24.090	ZB	44.333	CB	L
0431-08	NGC 1614	G	Sy2.0	SBc/Pec	0.0159	33.962	PBMP	21.594	PBMP			43.284	PBMP	Q
0433+29	3C 123	G			0.2180	34.736	RSEM	26.459	HR	25.350	ZB			L

TABLE 1 ... CONTINUED

object (1)	name (2)	ID (3)	class (4)	morph (5)	z (6)	L_{oiii} (7a)	ref (7b)	P5 (8a)	ref (8b)	PC5 (9a)	ref (9b)	Lx (10a)	ref (10b)	Remark (11)
0434-10	Mrk 618	G	Sy1.0		0.0346	34.841	W	21.226	UW3					Q
0438-08		G	Sy2.0	S0	0.0151	32.887	PBMP	20.971	PBMP			42.378	PBMP	Q
0440-00	NRAO 190	Q			0.8439	36.092	JB1	26.522	BM	26.500	BM			L
0442-28	PKS 0442-28	G	NLRG	E	0.1470	35.068	TMDF	25.280	MKT					L
0444-59	NGC 1672	G	Sy2.0	SBb	0.0044	32.940	PBMP	20.841	PBMP			41.418	PBMP	Q
0446-06	NGC 1667	G	Sy2.0	SBc	0.0152	33.802	PBMP	19.902	UW2			42.873	PBMP	Q
0450-03	NGC 1685	G	Sy2.0	SB0/a	0.0151	35.537	PBMP	20.620	UW2					Q
0450-18			Sy1.5		0.0585	33.421	DR	21.563	NED					Q
0505-37	NGC 1808	G	Sy2.0	(R)S(s)a	0.0033	31.831	PBMP	20.018	PBMP			41.579	PBMP	Q
0513-00	Mrk 1095	G	Sy1.0	S0/a	0.0327	34.644	W	21.050	NED			44.232	CB	Q
0518+16	3C 138	Q			0.7590	36.626	GW	27.152	BM	26.200	BM			L
0518-45	PIC A	G	BLRG	E	0.0350	34.535	TMDF	24.830	MKT	23.640	ZB	44.106	CB	L
0521-36	PKS 0521-36	G	BL Lac	N	0.0550	34.146	TMDF	25.000	MKT	24.170	ZB	43.753	CPPB	L
0538+49	3C 147	Q			0.5450	36.791	GW	27.117	BM	25.700	BM			L
0549-07	NGC 2110	G	Sy2.0	SB(r)a	0.0077	33.638	W	21.551	UW1			42.934	PBMP	Q
0551+46	MCG 8-11-11	G	Sy1.0	SB?	0.0210	35.064	DR	22.112	CFB					Q
0609+71	Mrk3	G	Sy2.0	S0?	0.0135	35.439	W	22.385	CFB			42.844	PBMP	Q
0637-75	06-71	Q			0.6510	36.854	TMDF	26.860	MKT			46.472	TWSS	L
0645+60	NGC 2273	G	Sy2.0	SB0/a	0.0077	33.927	W	20.587	UW1					Q
0645+74	IC 0450	G	Sy1.0	S0-a	0.0197	35.105	W	22.189	CFB			43.192	CPPB	Q
0655+54	Mrk 374	G	Sy1.2	S	0.0440	34.801	DR	21.612	UW3			43.830	CPPB	Q
0702+74	3C 173.1	G	NLRG		0.2920	34.635	RSEM	25.433	HR	23.440	ZB			L
0710+11	3C 175	Q			0.7680	36.964	JB1	26.414	BM	24.900	BM			L
0710+45	Mrk 376	G	Sy1.0	S0a	0.0560	34.876	DR	21.348	NED			44.714	CB	Q
0722-09	3C 178	G	Sy2.0	Sbc	0.0079	32.084	DR	21.849	TI					I
0734+80	3C 184.1	G	NLRG	cD?	0.1180	35.688	RSEM	24.782	HR	22.480	ZB			L
0736+01	OI 061	Q			0.1910	35.072	JB1	25.304	BM	25.300	BM			L
0737+65	Mrk 78	G	Sy2.0	SB0	0.0372	35.609	W	21.890	PBMP					Q
0738+31	OI 363	Q	Sy1.0		0.6300	36.372	JB1	26.421	BM	26.400	BM			L
0738+49	Mrk 79	G	Sy1.2	SBb	0.0231	34.937	W	20.870	UW3			43.294	CPPB	Q

TABLE 1 ... CONTINUED

object (1)	name (2)	ID (3)	class (4)	morph (5)	z (6)	L_{iii} (7a)	ref (7b)	P5 (8a)	ref (8b)	PC5 (9a)	ref (9b)	Lx (10a)	ref (10b)	Remark (11)
0742+31		Q			0.4620	36.755	B	25.984	PKDF					L
0745+56	DA240	G			0.0350	33.041	RSEM	23.482	HR	22.890	ZB			L
0754+39			Sy1.0		0.0964	35.853	S3	22.009	SMGM					Q
0800+60	Pri A	Q			0.6890	36.122	JB1	25.792	BSRF					L
0802+24	3C 192	G	NLRG	E1	0.0600	35.024	RSEM	24.436	HR	21.940	ZB			L
0804+27	Mrk 1212	G	Sy1.0		0.0412	33.448	DR	21.679	BKSD					Q
0804+39	Mrk 622	G	Sy2.0		0.0233	33.980	W	21.754	NED					Q
0804+76	PG 0804+76	Q			0.1000	35.147	BG	21.941	KSSS	21.521	KSSS	45.010	CB	Q
0806-10	3C 195	G	NLRG	N	0.1100	35.941	TMDF	24.870	MKT	23.390	ZB			L
0819+06	3C 198	G	NLRG	E	0.0820	34.449	SWCR	24.092	HOBL					L
0837-12	3C 206	Q			0.2000	35.764	JB1	25.000	JB2			45.252	TWSS	L
0838+13	3C 207	Q			0.6840	36.298	JB1	26.519	BM	25.900	BM			L
0840+50	NGC 2639	G		Sa?	0.0109	32.972	HFS	21.231	CFB					Q
0842-75		Q			0.5239	36.413	TMDF	26.270	MKT	25.900	MKT			L
0844+34	PG 0844+34	Q			0.0640	34.990	MRSE	20.657	KSSS			44.172	CPPB	Q
0851+17			Sy1.8		0.0643	35.024	DR	22.471	BKSD					Q
0858+29	3C 213.1	G	NLRG		0.1940	35.066	GW	25.102	HOBL					L
0859-25	PKS 0859-25	G	NLRG		0.3050	35.034	TMDF	25.880	MKT					L
0903+16	3C 215	Q			0.4110	35.835	JB1	25.517	BM	24.100	BM			L
0915-11	3C 218	G	Sy3.0	S0/cD2	0.0538	33.372	SWCR	25.160	MKT	23.410	ZB			L
0917+45	3C 219	G	NLRG		0.1740	35.340	RSEM	25.445	HR	23.780	ZB			L
0921+52	Mrk 110	G	Sy1.0	SB(r)	0.0362	35.107	W	21.242	KSSS	20.922	KSSS	43.849	CPPB	Q
0923+12	Mrk 705	Q	Sy1.0	(R)S0?	0.0287	34.562	MRSE	21.461	KSSS	20.899	MRS	43.850	CB	Q
0923+20	PG 0923+20	Q			0.1900	35.868	MRSE	21.548	KSSS			43.800	CPPB	Q
0923+39	4C 39.25	Q			0.6990	36.622	JB1	27.127	BM	27.100	BM			L
0926+79	3C 220.1	G			0.6100	36.000	JB2	25.992	HR	24.470	ZB			L
0934+01	PG 0934+01	G		E/S0	0.0500	34.612	MRSE	20.671	KSSS	20.232	KSSS	44.015	CPPB	Q
0936+36	3C 223	G	NLRG	E?	0.1370	35.616	RSEM	24.944	HR	22.762				L
0943-14	NGC 2992	G	Sy2.0	Sa/Pec	0.0077	34.367	W	21.195	UW1			42.634	PBMP	Q
0945+07	3C 227	G	BLRG	N	0.0860	35.161	SWCR	24.860	MKT	22.700	ZB			L

TABLE 1 ... CONTINUED

object	name	ID	class	morph	z	L_{iii}	ref	P5	ref	PC5	ref	Lx	ref	Remark
(1)	(2)	(3)	(4)	(5)	(6)	(7a)	(7b)	(8a)	(8b)	(9a)	(9b)	(10a)	(10b)	(11)
0945+73	4C 73.08	G			0.0581	34.315	RSEM	24.036	HR	22.370	ZB			L
0945-30	MCG-5-23-16	G	Sy2.0	S0	0.0082	33.834	PBMP	20.152	UW1			43.117	PBMP	Q
0947+39	PG 0947+39	Q			0.2060	35.403	MRSE	21.717	KSSS	21.545	KSSS	45.478	CPPB	Q
0952+09		Q			0.2980	36.081	B	24.744	NED					L
0953+25	OK 290	Q			0.7120	36.274	JB1	26.404	BM	26.400	BM			L
0953+41	PG 0953+41	Q			0.2389	35.918	BG	22.643	KSSS			45.322	CPPB	Q
0955+32		Q			0.5299	36.865	B	26.069	PKDF					L
0957-22	NGC 3081	G	Sy2.0	(R)SAB0	0.0083	34.581	W	19.338	UW2					Q
0958+29	3C 234	G	BLRG	N	0.1850	36.607	RSEM	25.332	HR	24.120	ZB			L
0958+55	NGC 3079	G	Sy3.0	SBC	0.0040	31.093	BWH	21.253	GC					I
1001+05	PG 1001+05	Q			0.1610	34.657	BG	21.901	KSSS			43.972	CPPB	Q
1003+35	3C 236	G	NLRG	E	0.0990	34.385	RSEM	24.704	HR	23.730	ZB			L
1004+13	PG 1004+13	Q			0.2399	35.813	JB1	25.111	BM	23.500	BM			L
1007+23	Mrk 716	G	Sy1.5	N	0.0574	34.405	DR	22.023	BKSD			44.343	CPPB	Q
1007+41	4C 41.21	Q			0.6110	36.758	JB1	26.230	BSRF					L
1011-04	PG 1011-04	Q			0.0579	34.854	MRSE	20.526	KSSS	20.628	KSSS	43.824	CPPB	Q
1012+00	PG 1012+00	Q			0.1850	35.684	MRSE	22.126	KSSS	21.940	KSSS	45.012	CPPB	Q
1020+20	NGC 3227	G	Sy1.5	SAB(r)a	0.0038	33.622	W	20.248	UW1			42.461	CB	Q
1020-10	OL-133	Q			0.1970	36.558	B	24.850	GWBE					L
1022+51	Mrk 142	G	Sy1.0	S0?	0.0449	34.235	W	20.420	KSSS			44.009	CPPB	Q
1028+31	OL 347	Q			0.1770	35.707	JB1	24.213	BM	24.000	BM			I
1029-34	NGC 3281	G	Sy2.0	SAB(rs+)a	0.0113	33.483	W	21.069	UW2					Q
1030+58	3C 244.1	G			0.4280	36.059	RSEM	25.930	HR	22.720 [†]	ZB			L
1030+60	Mrk 34	G	Sy2.0	SB0a	0.0505	35.886	W	21.734	PBMP					Q
1042+06	NGC 3362	G	Sy2.0	SABc	0.0277	34.359	PBMP	21.029	PBMP					Q
1048+34	PG 1048+34	Q			0.1670	35.348	MRSE	20.031	KSSS			44.872	CPPB	Q
1048-09	3C 246	Q			0.3440	36.031	MRSE	25.544	KSSS	24.340	KSSS			L
1049+61			Sy1.0		0.4220	36.665	S1	25.495	GC					L
1049-00	PG 1049-00	Q			0.3569	36.697	MRSE	22.429	KSSS			45.714	CPPB	Q
1100+77	3C 249.1	Q	BLRG		0.3110	36.635	JB1	25.552	BM	24.600	BM			L

TABLE 1 ... CONTINUED

object (1)	name (2)	ID (3)	class (4)	morph (5)	z (6)	L_{iii} (7a)	ref (7b)	P5 (8a)	ref (8b)	PC5 (9a)	ref (9b)	Lx (10a)	ref (10b)	Remark (11)
1103+72	NGC 3516	G	Sy1.5	(R)SB0/a	0.0104	34.352	W	20.204	UW1			42.992	CB	Q
1103-00	PG 1103-00	Q			0.4250	35.600	B	25.602	KSSS	24.682	KSSS	45.841	CPPB	L
1111+40	3C 254	Q			0.7340	36.957	JB1	26.407	BM	24.600	BM			L
1114+44	PG 1114+44	Q	Sy1.0		0.1439	35.666	MRSE	21.238	KSSS	21.153	KSSS	45.043	CPPB	Q
1115+40	PG 1115+40	Q			0.1540	35.339	MRSE	21.434	KSSS			44.157	CPPB	Q
1116+21	PG 1116+21	Q			0.1770	35.914	MRSE	22.532	KSSS	22.320	KSSS	45.010	CPPB	Q
1119+12	Mrk 734	Q	Sy1.0	S0/a	0.0491	34.848	MRSE	20.905	KSSS			44.411	CPPB	Q
1126-04	PG 1126-04	Q			0.0599	35.068	MRSE	20.816	KSSS			43.417	CPPB	Q
1129+53	Mrk 176	G	Sy2.0	Sa/Pec	0.0277	34.802	W	21.430	PBMP					Q
1133+21	Mrk 739	G	Sy1.0	S0/Pec	0.0296	34.064	DR	20.962	NED			43.722	CPPB	Q
1136-13	OM 16111-18	Q			0.5540	36.942	T MDF	26.450	MKT	25.700	SBMT			L
1136-37	NGC 3783	G	Sy1.0	(R)SB(r)a	0.0098	34.733	W	20.632	UW1			43.130	CB	Q
1137+32	NGC 3786	G	Sy1.8	Sa/Pec	0.0103	33.586	W	20.093	UW1			42.029	CPPB	Q
1137+66	3C 263	Q	BLRG		0.6460	36.958	JB1	26.259	HR	25.300	BM			L
1142+31	3C 265	G			0.8110	37.049	JB2	26.376	HR	24.810 [†]	ZB			L
1146-03		Q			0.3409	36.113	B	25.166	NED					L
1149-11	PG 1149-11	Q			0.0489	34.974	MRSE	21.344	KSSS	20.914	KSSS	44.165	CPPB	Q
1150+49	4C 29.45	Q			0.3339	35.486	B	25.732	PWP					L
1151-34	OM 38611-314	Q			0.2579	35.611	T MDF	25.880	MKT					L
1153+55	NGC 3982	G	Sy2.0	Sbc	0.0037	32.950	PBMP	19.013	UW2			41.727	CPPB	Q
1155+55	NGC 3998	G	Sy1.0	S0	0.0035	32.427	HFS	20.677	CFB					Q
1156+29		Q			0.7289	35.883	B	26.418	PK2					L
1200+44	NGC 4051	G	Sy1.0	SAB(r)bc	0.0024	32.985	W	19.072	UW1			41.684	CB	Q
1202+28	PG 1202+28	Q			0.1650	35.678	MRSE	21.939	KSSS	21.783	KSSS	44.934	CPPB	Q
1208+39	NGC 4151	G	Sy1.0	Sa/SBb	0.0033	34.735	W	20.743	CFB			42.274	CB	Q
1211+14	PG 1211+14	Q			0.0850	35.546	MRSE	23.615	KSSS	21.461	KSSS	44.420	CB	I
1214+07	NGC 4235	G	Sy1.0	SA(s)a	0.0044	32.301	W	19.546	UW1					Q
1215+30	NGC 4253	G	Sy1.0	(R)SB0/a	0.0127	34.677	W	20.927	UW3			43.346	CPPB	Q
1216+06	PG 1216+06	Q			0.3339	36.311	MRSE	23.285	KSSS	23.284	KSSS			Q
1216+47	NGC 4258	G	Sy1.0	Sb	0.0017	31.998	RSEM	20.485	CFB					Q

TABLE 1 ... CONTINUED

object (1)	name (2)	ID (3)	class (4)	morph (5)	z (6)	L_{oiii} (7a)	ref (7b)	P5 (8a)	ref (8b)	PC5 (9a)	ref (9b)	Lx (10a)	ref (10b)	Remark (11)
1216-10	PKS 1216-10	G			0.0870	35.010	SWCR	24.418	NED					L
1217+02	ON 029	Q			0.2399	36.163	JB1	25.020	BM	24.900	BM	45.373	TWSS	L
1219+75	Mrk 205	G	Sy1.0	Pec	0.0699	35.114	DR	21.244	SMGM			44.311	CB	Q
1223+12	NGC 4388	G	Sy2.0	Sb?	0.0083	34.164	W	20.561	CFB			43.119	PBMP	Q
1223+25	4C 25.40	Q			0.2680	35.996	JB1	24.514	BM	23.000	BM			L
1224+15	NGC 4419	G	Sy3.0	SBa	0.0156	32.487	BWH	21.456	S2					Q
1225+13	NGC 4438	G	Liner	S?	0.0036	33.440	RSEM	20.521	CFB					Q
1226+02	3C 273	Q			0.1580	36.475	TMDF	26.540	MKT	26.400	BM	45.923	CB	L
1228+12	3C 274	G	NLRG	E0-1	0.0040	32.395	K	23.503	CFB	22.339				L
1229+14	NGC 4501	G	Sy3.0	Sb	0.0066	32.736	BWH	21.043	S2					Q
1229+20	PG 1229+20	Q			0.0640	35.047	MRSE	20.992	KSSS	20.623	KSSS	44.662	CB	Q
1232+21	3C 274.1	G			0.4220	34.590	JB2	25.780	HR	23.930	ZB			L
1232-39	NGC 4507	G	Sy2.0	SB(r)ab	0.0119	34.829	W	21.030	PBMP			42.993	PBMP	Q
1235+12	NGC 4579	G	Sy3.0	SAB(r)b	0.0057	32.187	BWH	20.802	S2					Q
1237-05	NGC 4593	G	Sy1.0	(R)SBb	0.0093	33.818	W	19.686	UW1			43.213	CB	Q
1244+02	PG 1244+02	Q			0.0480	34.465	MRSE	20.830	KSSS	20.568	KSSS	43.847	CPPB	Q
1250+56	3C 277.1	Q			0.3200	36.262	GW	25.709	BM	24.000	BM			L
1253-05	3C 279	Q	Blazar		0.5360	36.077	TMDF	27.033	BM	27.000	BM	46.334	MEFK	L
1254+21	NGC 4826	G	Sy3.0	Sab	0.0013	30.484	BWH	19.525	S2					Q
1254+57	Mrk 231	G	Sy1.0	S?	0.0413	35.245	DR	23.388	CFB			43.306	CPPB	I
1258+28	5C 4.105	Q			0.6449	36.375	JB1	25.151	BM	25.100	BM			L
1300+16	Mrk 783	G	Sy1.0		0.0665	35.536	DR	21.677	UW3			43.947	CPPB	Q
1301-05	NGC 4941	G	Sy2.0	(R)Sab	0.0037	33.112	BWH	19.304	UW2					Q
1302-10	PG 1302-10	Q			0.2860	36.128	MRSE	25.427	KSSS	25.345	KSSS	45.581	CPPB	L
1305+06	3C 281	Q			0.5989	36.139	B	25.756	PK1					L
1306-09	PKS 1306-09	G	NLRG		0.4640	35.356	TMDF	26.270	MKT					L
1307+08	PG 1307+08	Q			0.1550	35.788	MRSE	21.507	KSSS			44.896	CB	Q
1308+27	3C 284	G	NLRG		0.2390	35.441	RSEM	25.131	HR	22.500	ZB			L
1308+37	NGC 5005	G	Sy2.0	SAB(r)bc	0.0036	31.621	DR	20.504	S2					Q
1309+35	PG 1309+35	Q			0.1840	35.972	MRSE	23.853	KSSS	23.773	KSSS	44.752	CPPB	I

TABLE 1 ... CONTINUED

object (1)	name (2)	ID (3)	class (4)	morph (5)	z (6)	L_{oiii} (7a)	ref (7b)	P5 (8a)	ref (8b)	PC5 (9a)	ref (9b)	Lx (10a)	ref (10b)	Remark (11)
1310-10	PG 1310-10	Q			0.0350	34.912	MRSE	20.047	KSSS			44.055	CPPB	Q
1311+36	NGC 5033	G	Sy1.9	SAc	0.0029	32.278	PBMP	18.977	UW2			41.230	PBMP	Q
1319+42	3C 285	G	NLRG		0.0790	34.162	RSEM	24.234	HR	22.150	ZB			L
1320+08	Mrk 1347	G	BL Lac	S	0.0502	33.877	DR	22.031	PG					Q
1322+65	PG 1322+65	Q			0.1680	34.959	BG	21.338	KSSS					Q
1322-29	NGC 5135	G	Sy2.0	Sab	0.0137	34.253	W	21.580	UW2					Q
1327+47	NGC 5194	G	Sy3.0	SABc/Pec	0.0018	31.956	BWH	20.600	NED					Q
1328+30	3C 286	Q	GPS		0.8490	36.911	GW	27.522	HOBL					L
1335+04	NGC 5252	G	Sy1.9	S0	0.0230	34.705	PBMP	21.519	PBMP			43.316	PBMP	Q
1336+48	NGC 5256	G	Sy2.0	Pec	0.0281	34.047	W	22.091	CFB			42.061	CPPB	Q
1338+30	Mrk 268	G	Sy2.0	S?	0.0399	34.684	W	21.978	PBMP					Q
1339+35	NGC 5273	G	Sy1.9	SA(s)0	0.0044	32.263	W	18.775	UW1					Q
1339+67	NGC 5283	G	Sy2.0	SAB0	0.0089	33.975	W	20.200	UW1					Q
1341+25	PG 1341+25	Q			0.0869	34.758	MRSE	20.139	KSSS			44.371	CPPB	Q
1342+56	Mrk 273	G	Sy2.0	S/Pec	0.0377	35.183	W	22.545	PBMP					Q
1345+12	4C 12.50	G		S0	0.1220	35.537	GW	25.172	HR					L
1346-30	IC 4329A	G	Sy1.0	S0/a/Pec	0.0138	34.449	BWH	21.197	ULWE			43.724	CB	Q
1350+31	3C 293	G		E6	0.0450	33.803	GW	24.133	CFB	22.840	ZB			L
1351+23	Mrk 662	Q			0.0550	34.478	DR	20.747	KSSS			43.527	CPPB	Q
1351+40	NGC 5353/4	G		S0+S0	0.0074	32.084	DR	20.817	CFB					Q
1351+64	PG 1351+64	Q			0.0869	35.803	DR	22.564	KSSS	22.714	KSSS	44.417	CPPB	Q
1351+69	Mrk 279	G	Sy1.0	SBb	0.0315	34.791	W	21.443	UW3			44.134	CB	Q
1352+18	PG 1352+18	Q			0.1580	35.153	MRSE	21.378	KSSS			44.312	CB	Q
1353+05	NGC 5363	G		I0?	0.0034	32.971	PBMP	20.683	CFB			40.304	PBMP	Q
1353+18		G	Sy2.0	Pec	0.0500	35.914	W	22.978	CFB					Q
1353+38	Mrk 464	G	Sy1.0		0.0504	35.264	W	21.733	UW3			44.582	CB	Q
1354+19	PKS 1354+19	Q			0.7189	37.010	B	26.619	SB					L
1355-41		Q			0.3129	36.049	TMDF	25.810	MKT	24.220	MKT			L
1402+26	PG 1402+26	Q			0.1640	35.745	MRSE	21.807	KSSS	21.618	MRS	45.220	CPPB	Q
1404+22	PG 1404+22	Q			0.0979	35.011	MRSE	21.547	KSSS	21.397	MRS	44.306	CPPB	Q

TABLE 1 ... CONTINUED

object (1)	name (2)	ID (3)	class (4)	morph (5)	z (6)	L_{iii} (7a)	ref (7b)	P5 (8a)	ref (8b)	PC5 (9a)	ref (9b)	Lx (10a)	ref (10b)	Remark (11)
1404+28	Mrk 668	G	Sy1.0		0.0797	35.025	DR	24.633	KTDD					L
1409+52	3C 295	G	BLRG		0.4610	35.181	RSEM	26.832	HOBL	24.050	ZB			L
1409-65	CIRCINUS	G	Sy2.0	Sb	0.0014	31.845	PBMP	20.611	PBMP			40.925	PBMP	Q
1410-02	NGC 5506	G	Sy1.9	SB0/a/Pec	0.0057	33.814	W	21.266	UW1			42.913	PBMP	Q
1411+44	PG 1411+44	Q			0.0890	35.046	BG	21.246	KSSS	21.148	KSSS	44.104	CPPB	Q
1415+25	NGC 5548	G	Sy1.5	(R)SA0/a	0.0179	34.913	W	20.952	ULWE			43.961	CB	Q
1415+45	PG 1415+45	Q			0.1140	33.748	BG	21.285	KSSS					Q
1416-12	PG 1416-12	Q			0.1289	35.481	MRSE	22.351	KSSS	21.659	KSSS	44.738	CB	Q
1420+19	3C 300	G	NLRG	E	0.2700	35.781	RSEM	25.513	HR	23.330	ZB			L
1425+26	PG 1425+26	Q			0.3660	36.461	BG	24.889	KSSS	24.282	KSSS	44.885	CPPB	L
1426+01	PG 1426+01	Q			0.0860	35.265	MRSE	21.512	KSSS	21.371	KSSS	43.557	CPPB	Q
1427+48	PG 1427+48	Q			0.2210	35.777	BG	20.592	KSSS			45.497	CPPB	Q
1429-43	NGC 5643	G	Sy2.0	Sbc	0.0040	33.741	W	20.544	PBMP			41.440	PBMP	Q
1431+05	NGC 5674	G	Sy1.9	Sb/bc	0.0249	34.565	PBMP	21.333	PBMP			43.437	PBMP	Q
1434+59	Mrk 817	G	Sy1.0	E/S0	0.0314	34.754	W	21.237	UW3			43.316	CPPB	Q
1435+36	NGC 5695	G	Sy2.0	SBb	0.0141	33.797	PBMP	20.313	PBMP			41.320	CPPB	Q
1435-06	PG 1435-06	Q			0.1289	35.212	MRSE	21.074	KSSS	21.057	KSSS			Q
1439+53	Mrk 477	G	Sy2.0	S0/a/Pec	0.0373	35.968	W	22.087	UW3					Q
1439-17	NGC 5728	G	Sy2.0	S(r)a/b	0.0099	34.469	W	20.199	UW2					Q
1440+35	PG 1440+35	Q			0.0770	34.800	BG	21.551	KSSS	21.170	KSSS	44.716	CB	Q
1441+52	3C 303	G	NLRG	E	0.1410	35.041	RSEM	24.893	HR	24.030	ZB			L
1444+40	PG 1444+40	Q			0.2669	34.673	BG	21.673	KSSS					Q
1448+27	PG 1448+27	Q			0.0649	34.929	BG	21.184	KSSS	21.197	KSSS	44.393	CPPB	Q
1448+63	3C 305	G		SB0	0.0410	34.819	GW	23.800	CFB	21.900	ZB			L
1501+10	Mrk 841	Q			0.0359	35.158	DR	20.833	KSSS	20.345	KSSS	43.661	CB	Q
1509-21		G	Sy1.0		0.0446	35.205	DR	22.189	NED					Q
1510-08	OR 107	Q			0.3610	35.981	TMDF	26.160	MKT	25.840	MKT			L
1512+37	PG 1512+37	Q			0.3709	36.277	BG	25.332	KSSS	24.473	KSSS			L
1514+07	3C 317	G		E	0.0342	33.338	SWCR	23.631	CFB	23.400	ZB			L
1514-24	ApLib	Q	BL Lac		0.0480	33.365	TMDF	24.190	MKT	24.070	MKT	43.496	CPPB	L

TABLE 1 ... CONTINUED

object	name	ID	class	morph	z	L_{iii}	ref	P5	ref	PC5	ref	Lx	ref	Remark
(1)	(2)	(3)	(4)	(5)	(6)	(7a)	(7b)	(8a)	(8b)	(9a)	(9b)	(10a)	(10b)	(11)
1519+22	PG 1519+22	Q			0.1369	34.264	BG	22.026	KSSS					Q
1522+15	MC 1522+155	Q			0.6280	36.009	B	25.652	BM	25.600	BM			L
1524+41	NGC5929/30	G	Sy2.0	E-S0+Sa	0.0086	33.473	W	20.924	CFB			40.691	CPPB	Q
1529+24	3C 321	G	NLRG	Pec	0.0961	35.000	GW	24.600	HR	23.000	ZB			L
1532+15	NGC 5953	G	Sy2.0	SAa/Pec	0.0075	33.299	BWH	20.842	NED					Q
1534+58	Mrk 290	G	Sy1.0	E	0.0317	35.388	W	20.829	KSSS	20.790	KSSS	43.978	CB	Q
1535+54	Mrk 486	Q	Sy1.0	(R)	0.0380	34.722	W	20.377	KSSS			43.272	CPPB	Q
1545+21	3C 323.1	Q	BLRG		0.2640	36.114	B	25.400	JB2	24.100	BM	44.944	CPPB	L
1547-79	B2 1547-79	G	BLRG		0.4830	36.508	TMDF	26.210	MKT	23.540 [†]	ZB			L
1549+20	3C 326	G	NLRG		0.0900	34.026	SWCR	24.269	HR	22.560	ZB			L
1549-79	PKS 1549-79	G	NLRG		0.1500	35.317	TMDF	25.530	MKT					L
1552+08	PG 1552+08	Q			0.1190	34.456	BG	21.625	KSSS					Q
1559+02	3C 327	G	NLRG		0.1040	35.072	SWCR	25.070	MKT	23.100	ZB			L
1602+01	3C 327.1	G	BLRG		0.4630	35.944	TMDF	26.110	MKT	24.870	ZB			L
1612+26	PG 1612+26	Q			0.1310	36.638	DR	22.514	KSSS	21.989	KSSS	45.171	CPPB	Q
1613+65	Mrk 876	Q		S0	0.1289	35.607	DR	22.277	KSSS	21.648	KSSS	45.203	CB	Q
1617+17	Mrk 883	Q			0.1140	34.835	DR	21.960	KSSS					Q
1618+17	3C 334	Q			0.5550	36.612	B	25.982	HOBL	25.200	BM			L
1622+23	3C 336	Q			0.9270	36.429	B	26.612	HOBL	25.000	BM			L
1622+41	Mrk 699	G	Sy1.0		0.0350	34.776	W	22.109	NED			43.977	CPPB	Q
1626+27	3C 341	G			0.4480	36.099	RSEM	25.672	HOBL	22.950	ZB			L
1626+55	PG 1626+55	Q			0.1330	34.969	BG	21.053	KSSS	21.287	KSSS	44.232	CPPB	Q
1627+24	Mrk 883	G	Sy2.0	S0/Pec	0.0380	34.635	W	22.028	BSRF					Q
1637+62	3C 343.1	G	GPS		0.7500	35.960	GW	26.520	HR	25.700 [†]	ZB			L
1637+82	NGC 6251	G	Sy2.0	E	0.0230	33.085	PBMP	23.254	PBMP					L
1637-77	PKS 1637-77	G			0.0427	33.761	TMDF	24.190	MKT	23.040	MKT			L
1641+17	3C 346	G		E	0.1610	34.590	GW	25.159	HR	24.330	ZB			L
1641+39	NGC 6212	G	Sy1.0	E	0.0313	33.193	W	20.835	NED					Q
1641+39	3C 345	Q			0.5940	36.177	JB1	27.014	BM	27.000	BM	46.202	M	L
1648+05	3C 348	G	NLRG		0.1540	33.812	TMDF	26.090	MKT	22.980	ZB			L

TABLE 1 ... CONTINUED

object	name	ID	class	morph	z	L _{oiii}	ref	P5	ref	PC5	ref	Lx	ref	Remark
(1)	(2)	(3)	(4)	(5)	(6)	(7a)	(7b)	(8a)	(8b)	(9a)	(9b)	(10a)	(10b)	(11)
1648-59	NGC 6221	G	Sy2.0	SBc	0.0044	32.732	W	20.882	NED					Q
1650+02	NGC 6240	G	Sy2.0	Im/Pec	0.0244	33.841	PBMP	22.222	PBMP					Q
1658+47	3C 349	G	NLRG		0.2050	34.887	RSEM	25.292	HOBL	23.558	FGGP			L
1701+31	Mrk 700	G	Sy1.9	S0/Pec	0.0349	33.847	DR	22.107	NED					Q
1704+60	3C 351	Q			0.3710	36.430	BG	25.800	JB2	24.900	BM	45.683	CPPB	L
1712-62	NGC 6300	G	Sy2.0	SBb(s)	0.0037	31.900	PBMP	20.294	PBMP			41.907	PBMP	Q
1717-00	3C 353	G		S0/E	0.0300	32.640	SWCR	24.850	MKT	22.750	ZB			L
1718-64	NGC 6328		Sy2.0		0.0142	34.343	PBMP	23.410	PBMP					L
1720+30	Mrk 506	G	Sy1.0	S(r)a	0.0431	35.035	W	22.119	BKSD			44.187	CB	Q
1733-56	PKS 1733-56	G	BLRG		0.0980	34.656	SWCR	25.080	MKT	24.380	ZB			L
1742+61	4C 61.34	Q			0.5230	36.225	JB1	25.855	BSRF					L
1807+69	3C 371	G	BL Lac		0.0500	34.165	GW	24.285	CFB	24.100		43.836	CPPB	L
1814-63	PKS 1814-63	G	NLRG		0.0630	33.911	SWCR	24.800	MKT					L
1828+48	3C 380	Q	GPS		0.6910	37.016	GW	27.220	BM	26.600	BM			L
1832+47	3C 381	G	BLRG	E	0.1610	34.833	RSEM	25.116	HR	22.720	ZB			L
1832-59			Sy2.0		0.0188	34.539	PBMP	21.907	NED			43.570	PBMP	Q
1833+32	3C 382	G	BLRG		0.0580	35.173	RSEM	24.435	HR	23.340	ZB	44.256	KKA	L
1842+45	3C 388	G			0.0910	33.786	RSEM	24.737	HR	23.244				L
1845+79	3C 390.3	G	BLRG	S0?	0.0560	35.726	RSEM	24.659	HR	23.590	ZB	44.419	CB	L
1907+50	NGC 6764	G	Sy3.0	SBbc	0.0080	33.010	DR	20.898	GC					Q
1928+73	4C 73.18	Q			0.3019	36.112	JB1	26.110	KPWS					L
1932-46	PKS 1932-46	G	NLRG		0.2310	35.574	T MDF	25.900	MKT	24.140 [†]	ZB			L
1934-63	PKS 1934-63	G	NLRG		0.1820	35.228	T MDF	25.940	MKT					L
1938-15	OV 164	G	BLRG		0.4519	35.899	T MDF	26.370	MKT					L
1939+60	3C 401	G			0.2010	34.401	RSEM	25.374	HR	23.740	ZB			L
1939-10	NGC 6814	G	Sy1.0	Sbc	0.0055	33.265	W	19.374	UW1			42.608	CB	Q
1949+02	3C 403	G	NLRG	S0	0.0590	34.779	SWCR	24.480	MKT	22.080	ZB			L
1954-38		Q			0.6300	36.349	T MDF	26.460	MKT	26.140	SBMT			L
2014-44	NGC 6890	G	Sy2.0	Sab	0.0080	33.721	W	19.965	UW2					Q
2021+61	OW 637	G	Sy2.0	E	0.2270	35.038	PBMP	25.676	PBMP					L

TABLE 1 ... CONTINUED

object (1)	name (2)	ID (3)	class (4)	morph (5)	z (6)	L_{oiii} (7a)	ref (7b)	P5 (8a)	ref (8b)	PC5 (9a)	ref (9b)	Lx (10a)	ref (10b)	Remark (11)
2041-10	Mrk 509	G	Sy1.0	E/S0	0.0345	35.631	W	21.274	ULWE			44.452	CB	Q
2048-57	IC 5063	G	Sy2.0	E/S0	0.0113	34.713	W	22.266	PBMP			42.744	PBMP	Q
2058-28	PKS 2058-28	G		E	0.0380	32.728	TMDF	24.010	MKT	22.590	ZB			L
2104-25	PKS 2104-25	G			0.0390	33.171	TMDF	24.320	MKT	21.840	ZB			L
2121+24	3C 433	G	Sy2.0	de	0.1016	34.721	S1	25.164	HR	22.240	ZB			L
2128-12	PKS 2128-12	Q			0.5010	36.666	TMDF	26.384	MKT					L
2130+09	IIZW 136	Q	Sy1.0	S0/a	0.0630	35.513	W	21.464	KSSS	21.246	KSSS	43.945	CB	Q
2135-14	PHL 1657	Q			0.2002	36.432	JB1	25.330	MKT	24.280	MKT	45.406	CB	L
2135-20	PKS 2135-20	G	BLRG		0.6350	36.377	TMDF	26.490	MKT					L
2141+17	OX 169	Q	Sy1.0		0.2130	35.553	JB1	25.288	BSRF					L
2141+27	3C 436	G			0.2140	34.925	RSEM	25.255	HR	23.460	ZB			L
2143-15	OX 173	Q			0.6999	35.884	JB1	26.132	GWBE					L
2152-69	PKS 2152-69	G	BLRG	E	0.0270	34.086	TMDF	24.510	MKT	23.010	ZB			L
2153+37	3C 438	G			0.2900	35.041	RSEM	25.761	HR	23.570	ZB			L
2201+31	4C 31.63	Q			0.2980	35.701	JB1	25.913	BM	25.700	BM			L
2203-18	22-11	Q			0.6179	36.078	TMDF	26.850	MKT	26.560	SBMT			L
2209+18	PG 2209+18	Q			0.0700	34.431	BG	23.708	KSSS	23.671	KSSS	44.204	CPPB	L
2211-17	3C 444	G	NLRG		0.1530	33.626	TMDF	25.320	MKT	23.820	ZB			L
2214+13	Mrk 304	Q	Sy1.0		0.0658	35.060	W	20.571	KSSS			43.763	CPPB	Q
2221-02	3C 445	G	BLRG	N	0.0560	35.392	TMDF	24.430	MKT	23.000	ZB	44.634	P	L
2233+13	PG 2233+13	Q			0.3249	35.644	BG	22.338	KSSS	22.028	KSSS	44.859	CPPB	Q
2233-26	NGC 7314	G	Sy1.9	Sbc	0.0046	32.763	W	19.157	PBMP			42.431	PBMP	Q
2234+28	CTD 135	Q			0.7950	35.900	JB1	26.902	BM	26.900	BM			L
2243+39	3C 452	G		E	0.0810	34.587	RSEM	24.898	HR	23.460	ZB			L
2243-12	OY 172	Q			0.6300	36.329	TMDF	26.590	MKT	26.540	SBMT			L
2250-41	PKS 2250-41	G			0.3100	35.940	TMDF	25.750	MKT	23.120 [†]	ZB			L
2251+11	PG 2251+11	Q			0.3230	36.453	JB1	25.414	BM	23.900	BM	45.634	CPPB	L
2251+15	3C 454.3	Q			0.8600	37.134	JB1	27.527	BM	27.500	BM	46.907	M	L
2251-17			Sy2.0		0.0683	33.509	S3	21.701	NED			44.782	CB	Q
2252+12	3C 455	Q	GPS		0.5430	36.310	GW	26.038	HR					L

TABLE 1 ... CONTINUED

object (1)	name (2)	ID (3)	class (4)	morph (5)	z (6)	L_{oiii} (7a)	ref (7b)	P5 (8a)	ref (8b)	PC5 (9a)	ref (9b)	Lx (10a)	ref (10b)	Remark (11)
2258-13	NGC 7450	G	Sy2.0	(R)E/S0	0.0103	33.745	W	19.796	UW1					Q
2300+08	NGC 7469	G	Sy1.2	(R)SBa	0.0165	34.838	W	21.786	ULWE			43.773	CB	Q
2301+22	Mrk 315	G	Sy1.0	E0/Pec	0.0388	34.653	W	21.569	NED			43.713	CPPB	Q
2302-08	Mrk 926	G		S0/a	0.0049	33.492	DR	20.754	ULWE			42.504	CB	Q
2304+04	PG 2304+04	Q			0.0419	34.629	BG	20.679	KSSS	20.821	KSSS	44.121	CPPB	Q
2308+09	PG 2308+09	Q			0.4320	36.002	BG	25.416	KSSS	24.757	KSSS	46.275	CPPB	L
2309+18	3C 457				0.4280	35.726	RSEM	25.625	HR					L
2314+03	3C 459	G	NLRG	N	0.2200	35.398	TMDF	25.440	MKT	25.360	ZB			L
2315-42	NGC 7582	G	Sy2.0	(R)SBb	0.0052	33.627	W	20.822	UW1			41.861	PBMP	Q
2316-00	NGC 7603	G	Sy1.5	SAb/Pec	0.0291	34.253	W	21.512	NED			43.545	CPPB	Q
2325+08	NGC 7674	G	Sy2.0	SBb	0.0289	35.259	W	22.303	CFB			43.486	PBMP	Q
2326+03	NGC 7682	G	Sy2.0	SB(r)ab	0.0171	34.467	W	21.436	PBMP			43.052	CPPB	Q
2329+28	Mrk 930		Sy2.0		0.0191	33.502	PBMP	21.101	BKSD					Q
2344+09	PG 2344+09	Q			0.6769	37.339	JB1	26.405	BM	26.400	BM	46.867	CPPB	L
2345-16	OZ 176	Q			0.5759	36.186	JB1	26.680	MKT	26.490	SBMT			L
2349-01		G	Sy1.0	E?	0.1745	35.710	S1	24.917	PK2					L
2353+28	4C 28.59	Q			0.7310	35.631	JB1	25.949	NED					L
2353+29	CGCG 498-038		Sy2.0		0.0307	35.160	PBMP	22.415	PBMP			44.307	PBMP	Q
2356-61	PKS 2356-61	G	NLRG	E3	0.0960	35.217	TMDF	25.220	MKT	23.100	ZB			L

NOTE 0.– † upper limit

NOTE 1.– The columns list (1) IAU name; (2) name frequently referred to; (3) identification: G = galaxy, Q = quasar; (4) AGN classification: Sy = Seyfert Galaxy, NLRG = Narrow Line Radio Galaxy, BLRG = Broad Line Radio Galaxy, GPS = GHz Peaked Radio Galaxy; (5) morphological type of the host galaxy; (6) redshift; (7a,b) $\log [\text{O III}]$ 5007 line luminosity (in Watts) and corresponding reference; (8a,b) \log total 5 GHz radio power (in W/Hz/Sr) and corresponding reference; (9a,b) \log core 5 GHz radio power (in W/Hz/Sr) and corresponding reference; (10a,b) \log 2–10 keV X-ray luminosity (in erg/s) and corresponding reference; (11) remarks: L = radio-loud, Q = radio-quiet, I = intermediate.

NOTE 2.– References for Table 1: B: Brotherton 1996; BG: Boroson 1992; BKSD: Bica 1995; BSB: Brinkmann 1994; BSRF: Brinkmann 1996; BWH: Braatz 1997; CB: Ceballos 1996; CFB: Condon 1991; CPPB: Ceca 1990; DR: Dahari 1988; FGGP: Feretti 1984; FMTL: Fabbiano 1984; GC: Gregory 1991; GFGP: Giovannini 1988; GW: Gelderman 1994; GWBE: Griffith 1994; HFS: Ho 1993; HOBL: Heckman 1994; HR: Herbig 1992; JB1: Jackson 1991; JB2: Jackson 1990; KKA: Kaastra 1991; KPWS: Kuhr 1981; KSSS: Kellermann 1989; KTDD: Kojoian 1980; LRL: Laing 1983; MKT: Morganti 1993; MRS: Miller 1993; MRSE: Miller 1992; NED: NASA Extragalactic Database; P: Pounds 1990; PBMP: Polletta 1996; PG: Padovani 1995; PK1: Pauliny-Toth 1968; PK2: Pauliny-Toth 1972a; PKDF: Pauliny-Toth 1972b; PSSE: Perlman 1996; PWP: Pauliny-Toth 1978; RMFV: Rush 1996; RMGB: Rothschild 1983; RSEM: Rawlings 1989; S1: Steiner 1981; S2: Sramek 1975; SB: Shimmins 1972; SBMT: Siebert 1996; SBW: Shimmins 1975; SMG1: Stocke 1990; SMG2: Stocke 1991; SWCR: Simpson 1996; TI: Tabara 1980; TMDF: Tadhunter 1993; TWSS: Turner 1989; ULWE: Unger 1987; UM: Ulrich 1984; UW1: Ulvestad 1984a; UW2: Ulvestad 1989; UW3: Ulvestad 1984b; W: Whittle 1992; ZB: Zirbel 1995